Research Paper

Prognostic value of prostaglandin I2 synthase and its correlation with tumor-infiltrating immune cells in lung cancer, ovarian cancer, and gastric cancer

Danian Dai[1,2,*], Bo Chen[3,*], Yanling Feng[1,2,*], Weizhong Wang[4], Yanhui Jiang[1,2], He Huang[2], Jihong Liu[1,2]

[1]Department of Gynecology and Obstetrics, The Fifth Affiliated Hospital of Sun Yat-Sen University, Zhuhai 519000, Guangdong, China
[2]Department of Gynecologic Oncology, State Key Laboratory of Oncology in South China, Collaborative Innovation Center for Cancer Medicine, Sun Yat-Sen University Cancer Center, Guangzhou 510060, Guangdong, China
[3]Department of Breast Cancer, Cancer Center, Guangdong Provincial People's Hospital and Guangdong Academy of Medical Sciences, Guangzhou 510080, Guangdong, China
[4]Department of Respiratory Medicine, The First Affiliated Hospital of University of South China, Hengyang 421001, Hunan, China
*Equal contribution

Correspondence to: Jihong Liu, He Huang; **email:** liujih@mail.sysu.edu.cn, huangh@sysucc.org.cn
Keywords: prostaglandin I2 synthase, tumor-associated macrophages, prognosis, lung cancer, ovarian cancer
Received: December 16, 2019 **Accepted:** April 27, 2020 **Published:** May 28, 2020

ABSTRACT

Background: Prostaglandin I2 synthase (PTGIS) is a crucial gene for the synthesis of prostaglandin I2, which has multiple roles in inflammation and immune modulation. However, studies on the prognostic value of PTGIS and its correlation with tumor-infiltrating immune cells in multiple cancers are still rare.

Results: Multiple datasets of the Oncomine database showed that PTGIS was expressed at low levels in lung cancer and ovarian cancer compared to the levels in normal tissues. Kaplan-Meier plotter showed that high PTGIS was associated with poor overall survival and progression-free survival in lung, ovarian, and gastric cancers. Moreover, PTGIS expression was significantly positively correlated with infiltrating levels of macrophages and was strongly associated with a variety of immune markers, especially tumor-associated macrophages (TAMs) and T-regulatory cells (Tregs).

Conclusions: High expression of PTGIS could promote the infiltration of TAMs and Tregs in the tumor microenvironment and deteriorate outcomes of patients with lung, ovarian, and gastric cancers. These findings suggest that PTGIS could be taken as a potential biomarker of prognosis and tumor-infiltrating immune cells.

Methods: PTGIS expression was investigated in different datasets of the Oncomine database, and its expression levels in various tumors and corresponding normal tissues were analyzed by the Tumor Immune Estimation Resource (TIMER). Then, the clinical prognostic value of PTGIS was assessed with online public databases. In addition, we initially explored the correlation between PTGIS and tumor-infiltrating immune cells by TIMER and Gene Expression Profiling Interactive Analysis (GEPIA).

INTRODUCTION

Solid tumors are the most extensive and common malignant tumors worldwide, including lung tumors, ovarian tumors, and gastric tumors. Insidious onset, invasive and fast growth, and high recurrence and metastasis rates are common characteristics leading to poor prognosis [1]. Recently, immunotherapy has been widely used in the treatment of solid tumors, including melanoma and lung, ovarian, breast, and stomach cancers, and its tolerable toxicity and long-term survival improvement have benefited many advanced cancer patients, leaving immunotherapy as the most promising direction for curing cancer [2]. Some immunotherapies, such as programmed death-1 (PD-1) and programmed death ligand-1 (PD-L1) inhibitors or cytotoxic T lymphocyte-associated antigen 4 (CTLA4) therapies, have shown an optimistic antitumor effect in melanoma [3, 4], lung cancer [5], gastrointestinal cancer [6] and ovarian cancer [7]. However, the current anti-CTLA-4 agent showed no effect in a clinical study of prostate cancer [8], and anti-PD1 therapy showed less effect in colorectal cancer [9] and even promoted tumor progression for some patients with murine double minute2 (MDM2) amplification or epidermal growth factor receptor (EGFR) aberration [10]. Moreover, increasing evidence has demonstrated that tumor-infiltrating immune cells interact with tumor cells and immunotherapy and have important implications for efficacy and patient outcomes [11–13]. Therefore, the elucidation of the mechanism of the interaction between tumor phenotype and infiltrating immune cells in the microenvironment and the exploration of new immune-related therapeutic targets are urgent for the treatment of solid tumors.

Prostaglandin I2 synthase (PTGIS) is a protein-encoding gene localized on chromosome 20q13.11-q13.13 and was first reported in 1996 [14]. PTGIS encodes a member of the cytochrome P450 superfamily, a monooxygenase that catalyzes the metabolism of many drugs and the synthesis of lipids such as cholesterol and steroids. In addition, PTGIS could be involved in iron and heme metabolism, oxidative stress, xenobiotic and drug metabolism, glutathione and prostaglandin metabolism, and the conversion of prostaglandin H2 to prostaglandin I2 (PGI2) [14, 15]. A previous study observed that hypermethylation of the PTGIS promotor was associated with diminished gene expression in colorectal carcinogenesis [16]. Furthermore, other studies suggested that PTGIS variants may affect breast cancer susceptibility [17], and elevated PTGIS was associated with liver metastasis and poor survival outcomes for patients with colon cancer [18]. These findings suggest that PTGIS has distinctly essential impacts on tumorigenesis, progression, and metastasis.

PGI2 is an important product of the arachidonic acid (AA) metabolism pathway, and PTGIS is one of the key enzymes. PGI2 is involved in inflammatory responses and activation of CD4+ T cells during physiological processes [19]. In addition, PGI2 is a crucial immunoregulatory lipid mediator that affects the differentiation of Th17 cells and T-regulatory cells (Tregs) [20]. The above results suggest that PTGIS has an indirect regulatory effect on microenvironment immune cells. Nevertheless, the potential functions and mechanisms of PTGIS in tumorigenesis and development and the immune microenvironment are undefined.

In this study, our aim was to comprehensively analyze the relationship between the expression of PTGIS and prognosis in cancer patients and to explore the correlation between PTGIS and tumor-infiltrating immune cells. Our findings provide new ideas for elucidating the potential mechanism of PTGIS in tumor progression and the mechanism by which PTGIS is associated with tumor-infiltrating immune cells.

RESULTS

PTGIS expression level in various kinds of tumors

To investigate the expression levels of PTGIS, the PTGIS mRNA levels in various tumors and normal samples were analyzed with the Oncomine database. Across various cancer types, significantly more datasets showed low expression of PTGIS in cancer samples versus normal samples than overexpression of PTGIS (Figure 1A). The expression of PTGIS was absolutely lower in bladder cancer, cervical cancer, colorectal cancer, head and neck cancer, leukemia, lung cancer, ovarian cancer, and prostate cancer than in normal samples. In addition, higher expression was found in pancreatic cancer and other cancer samples than in the corresponding normal samples, and the expression levels in some cancers were controversial. The specific data of PTGIS mRNA expression levels in various cancer datasets are displayed in Supplementary Table 1. Next, we further examined PTGIS expression in multiple human cancers with RNA-seq data from The Cancer Genome Atlas (TCGA). The expression levels of PTGIS between tumor and matched normal tissues in all TCGA datasets are shown in Figure 1B. Taken together, the data confirmed that the PTGIS gene was downregulated in multiple cancers compared to normal samples.

Prognostic value of PTGIS in cancers

To explore the correlation between PTGIS expression and prognosis in human cancers, we investigated the

effects of PTGIS expression on survival via PrognoScan. Eight out of thirteen cancers showed a potential correlation between PTGIS and prognosis (Supplementary Table 2). Interestingly, compared with low PTGIS expression, high expression of PTGIS indicated a better survival prognosis for overall survival (OS) (hazard ratio [HR]=0.63, 95% confidence interval [CI]=0.44 to 0.90, P=0.012) and disease specific survival (DSS) (HR=0.60, 95% CI=0.40 to 0.90, P=0.013) in breast cancer (Figure 2A and 2B). However, among the other three common solid tumors (colorectal cancer, ovarian cancer, and lung cancer), high PTGIS expression was associated with a worse prognosis than low PTGIS expression (Figure 2C–2H). In addition, PTGIS had no significant effect on OS in colorectal cancer. The survival plots generated from different datasets are shown in Supplementary Figure 2.

Then, we further assessed the prognostic value of PTGIS in tumors with the Kaplan-Meier plotter, which is based on Affymetrix microarray data. Notably, PTGIS had less influence on OS in this analysis than it had been shown to have in the PrognoScan analysis for breast cancer (HR=0.89, 95% CI=0.72 to 1.1, P=0.28) (Figure 3A), and high PTGIS expression was correlated with poor prognosis in gastric cancer (OS HR=2.03, 95% CI=1.69 to 2.44, P=7.8e-15; progression-free survival [PFS] HR=2.05, 95% CI=1.65 to 2.54, P=2.5e-11) (Figure 3C and 3D). Consistent with previous results, patients with high expression of PTGIS had a poor prognosis in both lung cancer (OS HR=1.47, 95% CI=1.28 to 1.69, P=4.8e-08; PFS HR=2.13, 95% CI=1.74 to 2.6, P=3.5e-14) and ovarian cancer (OS HR=1.23, 95% CI=1.08 to 1.4, P=0.002; PFS HR=1.26, 95% CI=1.11 to 1.43, P=3.1e-4) (Figure 3E–3H). Based on this large-sample validation analysis, these results suggest that high PTGIS expression implies reduced survival in ovarian, lung and gastric cancer.

The above analyses of PTGIS were based on microarray data from Kaplan-Meier plotter and the PrognoScan database. The prognostic value of PTGIS was explored for various tumors with RNA-seq data from TCGA with the Gene Expression Profiling Interactive Analysis (GEPIA) website. A total of 33 cancer types were included in the analysis of the relationship between PTGIS expression and survival (Supplementary Figure 3). Compared with downregulated PTGIS expression, elevated PTGIS expression was associated with worse OS or disease free survival (DFS) in ACC (adrenocortical carcinoma), BLCA (bladder urothelial carcinoma), COAD (colon adenocarcinoma), GBM (glioblastoma multiforme), KIRP (kidney renal papillary cell carcinoma), LUSC (lung squamous cell carcinoma), OV (ovarian serous cystadenocarcinoma) and STAD (stomach adenocarcinoma). In addition,

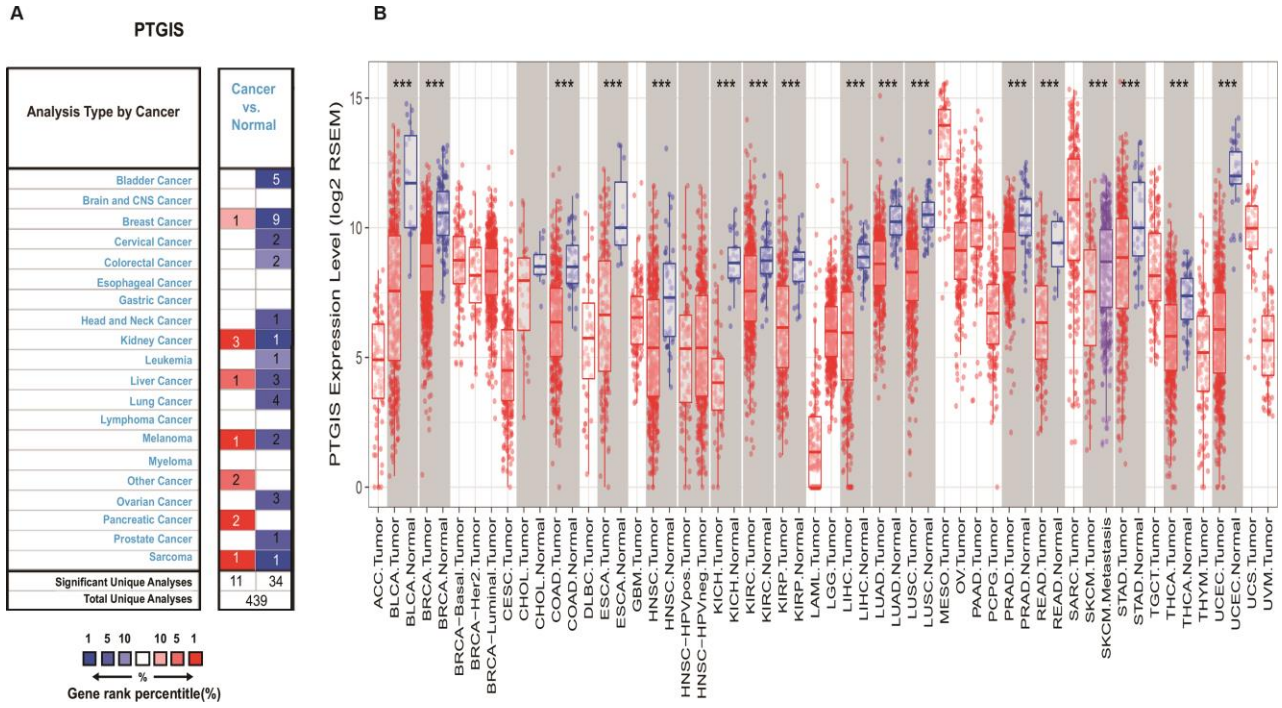

Figure 1. Expression of PTGIS in various human tumors. (**A**) Increased or decreased expression of PTGIS in different tumors compared to normal tissues in the Oncomine database. (**B**) PTGIS expression of different tumor types from the TCGA database was investigated by TIMER (*P < 0.05, **P < 0.01, ***P < 0.001).

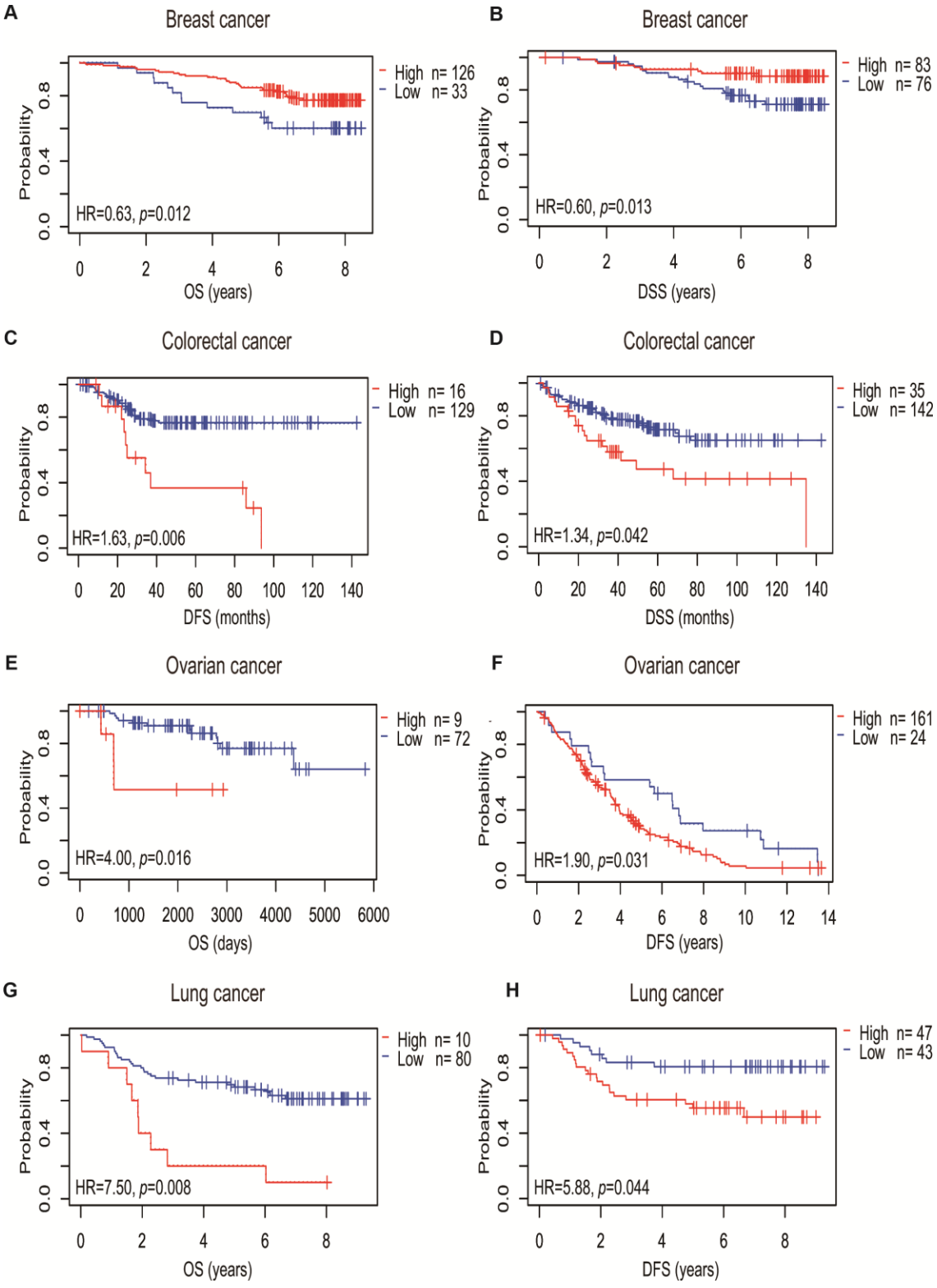

Figure 2. Survival curves of high or low expression of PTGIS in different tumors from the PrognoScan database. (**A**, **B**) High PTGIS expression was correlated with better OS and DSS than low PTGIS expression in the breast cancer cohort [GSE1456-GPL96 (n = 159)]. (**C**, **D**) High PTGIS expression was correlated with poorer DFS (n = 145) and DSS (n = 177) than low PTGIS expression in the colorectal cancer cohort (GSE17536). (**E**, **F**) High PTGIS expression was correlated with poorer OS and DFS than low PTGIS expression in two ovarian cancer cohorts [GSE8841 (n = 81) and GSE26712 (n = 185)]. (**G**, **H**) High PTGIS expression was correlated with poorer OS and DSS than low PTGIS expression in a lung cancer cohort (GSE14814, n = 90). OS, overall survival; DFS, disease-free survival; DSS, disease-specific survival.

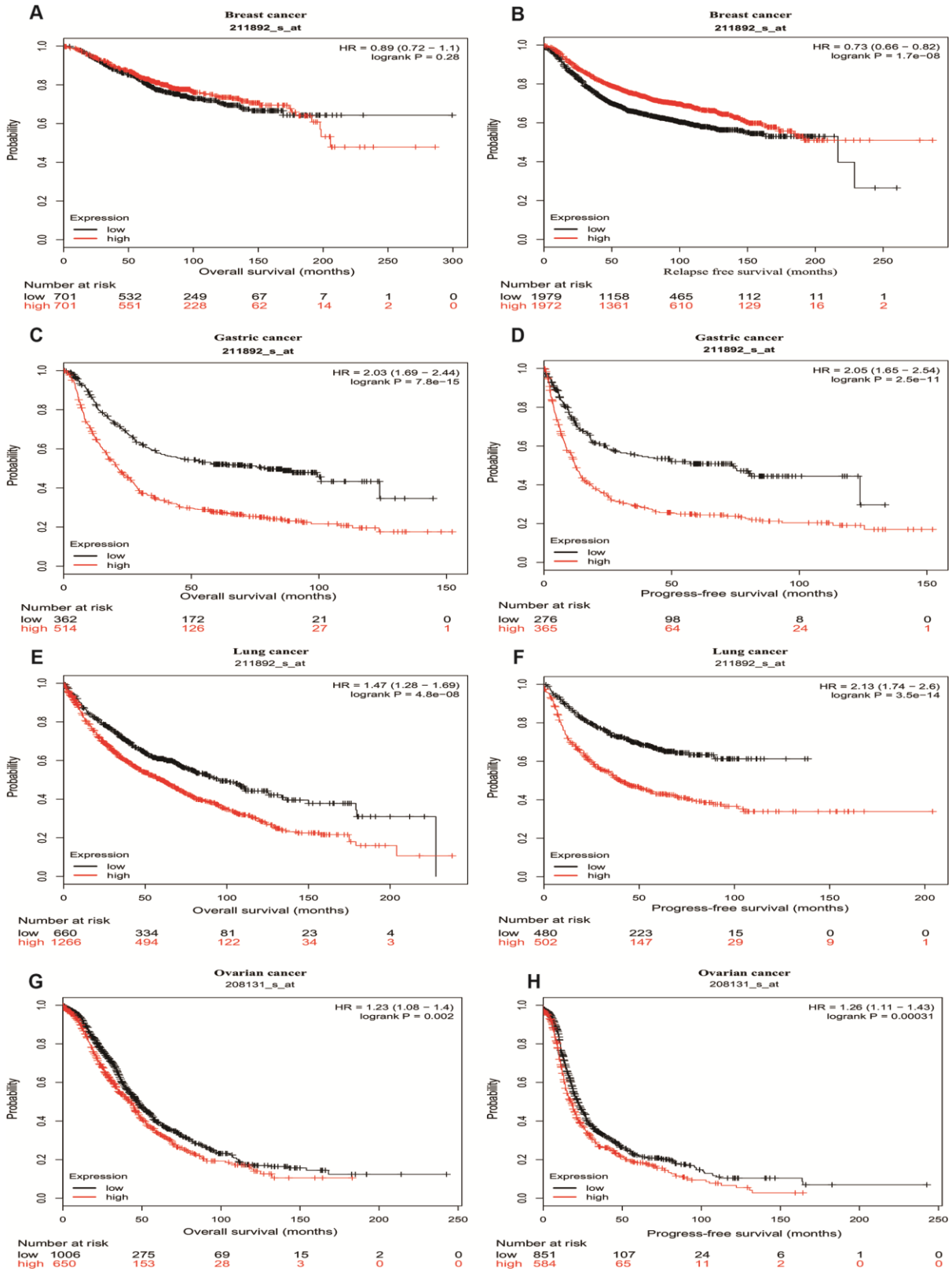

Figure 3. Survival curves of high or low expression of PTGIS in different tumors from Kaplan-Meier plotter. (**A**, **B**) OS and DFS survival curves of breast cancer (n = 1,402 and n = 3,951, respectively). (**C**, **D**) OS and PFS survival curves of gastric cancer (n = 876 and n = 641, respectively). (**E**, **F**) OS and PFS survival curves of lung cancer (n = 1,926 and n = 982, respectively). (**G**, **H**) OS and PFS survival curves of ovarian cancer (n = 1,656 and n = 1,435, respectively). OS, overall survival; PFS, progression-free survival; DFS, disease-free survival.

elevated PTGIS expression was associated with improved DFS for only SARC (sarcoma). These results demonstrate the important prognostic value of PTGIS as an oncogene in certain types of cancer, suggesting that it plays a crucial role in the progression of cancer.

High expression of PTGIS deteriorates the outcomes of ovarian and gastric cancer patients with lymph node metastasis

To explore the potential mechanism by which PTGIS expression affects prognosis, we studied the association between expression levels of PTGIS and clinical variables in ovarian (Supplementary Table 3) and gastric cancer patients (Supplementary Table 4). For serous ovarian cancer, high expression of PTGIS was related to reduced OS and PFS. Specifically, compared with low PTGIS mRNA expression, high PTGIS mRNA expression was correlated with worse OS and PFS only in stage 3 disease (OS HR = 1.2, P = 0.0398; PFS HR = 1.28, P = 0.0025), which includes involvement of retroperitoneal lymph nodes [21]. In addition, PTGIS high expression alone did not impair the OS of patients treated with optimal debulking surgery. For gastric cancer patients, compared with lower levels of PTGIS, elevated PTGIS was correlated with worse OS and PFS after stratification by HER2 status, Lauren classification, or differentiation (P < 0.05). Moreover, PTGIS expression had a significant prognostic correlation with the N stage. Stages N0-4 indicate different degrees of regional lymph node metastasis [22]. The above results imply that the expression level of PTGIS can deteriorate the prognosis of patients with ovarian or gastric cancer with lymph node metastasis.

The expression level of PTGIS is positively correlated with infiltrating immune cells in lung, ovarian and gastric cancers

Tumor-infiltrating lymphocytes (TILs) are associated with sentinel lymph node metastasis and prognosis in tumors [23–25]. Thus, the correlation between PTGIS and tumor-infiltrating immune cells was assessed in different cancers with TIMER. We observed that PTGIS expression levels were significantly associated with tumor purity in 26 kinds of cancer, of which 23 kinds of cancer showed a negative correlation between PTGIS expression and tumor purity. In addition, PTGIS expression was significantly correlated with infiltrating immune cells, including B cells, CD4+/CD8+ T cells, macrophages, neutrophils, and dendritic cells, in various types of cancers (Figure 4 and Supplementary Figure 4). After the preliminary analysis of the correlation between PTGIS and infiltrating immune cells in various cancers, we then selected the specific cancers in which PTGIS was correlated with oncologic outcomes and infiltrating immune cells. It was reported that the tumor purity level had an impact on immune infiltration in an analysis of clinical sample data based on genetic testing [26, 27]. TIMER and GEPIA have most of the common transcriptomics data derived from the TCGA database [28, 29], so we selected the types of cancer in TIMER in which PTGIS had a significantly negative correlation with tumor purity and prognostic significance in GEPIA. Based on the prognostic results related to PTGIS from the PrognoScan, Kaplan-Meier-plotter and GEPIA analyses, we eventually selected LUSC, OV and STAD for further research on immune infiltration via TIMER. The PTGIS expression level had a significant negative correlation with tumor purity but significant positive correlations with the levels of 6 infiltrating immune cells in LUSC (Figure 4A). However, there were significantly negative correlations with tumor purity (r = -0.481, P = 2.01e-29) and the level of infiltrating B cells (r = -0.168, P = 2.15e-04) and a positive correlation with only macrophages (r = 0.134, P = 3.23e-03) in OV (Figure 4B). Interestingly, there was no significant correlation with tumor purity (r = -0.045, P = 3.77e-01) and the level of infiltrating B cells (r = -0.09, P = 8.42e-02) but significant positive correlations with the levels of infiltrating CD8+ T cells (r = 0.25, P = 1.13e-06), CD4+ T cells (r = 0.477, P =3.63e-22), macrophages (r = 0.638, P = 1.12e-43), neutrophils (r = 0.218, P = 2.30e-05), and DCs (r = 0.443, P = 2.68e-19) in STAD (Figure 4C). These findings strongly demonstrate that PTGIS could recruit immune cells in the tumor microenvironment (TME) in LUSC, OV and STAD, especially on macrophages.

Correlation analysis between PTGIS and markers of infiltrating immune cells

To explore the effects of PTGIS expression on tumor-infiltrating immune cells, we analyzed the relationships between PTGIS expression and various markers of immune cells in LUSC, OV, and STAD via public databases. We selected some of the infiltrating immune cells, including innate immune cells (Supplementary Table 5) and adaptive immune cells (Supplementary Table 6), and analyzed the relationship between PTGIS and specific markers of these immune cells in LUSC, OV and STAD (Figure 5). In LUSC and STAD, the changes in correlation coefficients between the expression level of PTGIS and the expression of gene marker sets of different immune cells were not significant after adjustment for purity. However, the association between PTGIS and immune markers changed dramatically in OV. It is worth noting that the correlation between PTGIS and various immune cell markers was significantly increased without adjustment for purity.

Specifically, we found that PTGIS expression was more highly correlated with gene markers of monocytes/macrophages (monocytes, TAMs, and M2 macrophages) than with gene markers of other infiltrating immune cells in LUSC, OV and STAD (Supplementary Table 5). In addition, we determined the correlation coefficients between PTGIS and specific markers of monocytes, TAMs, M1 macrophages, and M2 macrophages in LUSC, OV and STAD (Figure 5). We further investigated the relationship between PTGIS and the above gene markers of immune cells in normal tissues and tumors using the GEPIA database. Notably, there was no correlation between PTGIS and most immune markers of monocytes and TAMs in normal lung tissues. The results of the correlation were generally consistent with those of the TIMER analysis in tumors (Supplementary Table 7). These results imply that PTGIS likely plays a promoting role in the regulation of macrophage polarization in LUSC, OV, and STAD.

Elevated PTGIS expression levels were associated with a high degree of Tregs infiltration in LUSC, OV and STAD, and Tregs markers such as FOXP3, STAT5B, TGFB1, and IL2RA also showed obvious correlations with PTGIS expression (Supplementary Table 6). These results suggest a strong positive correlation between PTGIS and Tregs infiltration. There is evidence that Tregs can negatively regulate CD8+ T cell and natural killer cell responses to tumor cells as well as promote angiogenesis and metastasis [30]. Whether PTGIS is a pivotal factor that activates Tregs and tumor progression still needs further study.

Furthermore, we also observed a significant positive correlation between PTGIS and some of the markers of Tregs and T cell exhaustion, including FOXP3, STAT5B, TGFB1 (TGFβ), IL2RA (CD25), and HAVCR2 (TIM-3), in LUSC, OV, and STAD. FOXP3 has a crucial role in the development and function of Tregs, and excessive Tregs could prevent the immune system from destroying cancer cells and promote cancer progression [31]. Interestingly, PTGIS expression also has a positive correlation with TIM-3, an important gene mediating T cell exhaustion and macrophage activation; the presence of the exhausted phenotype downregulates the immune response in tumor-bearing hosts [32, 33]. Therefore, these results further confirm

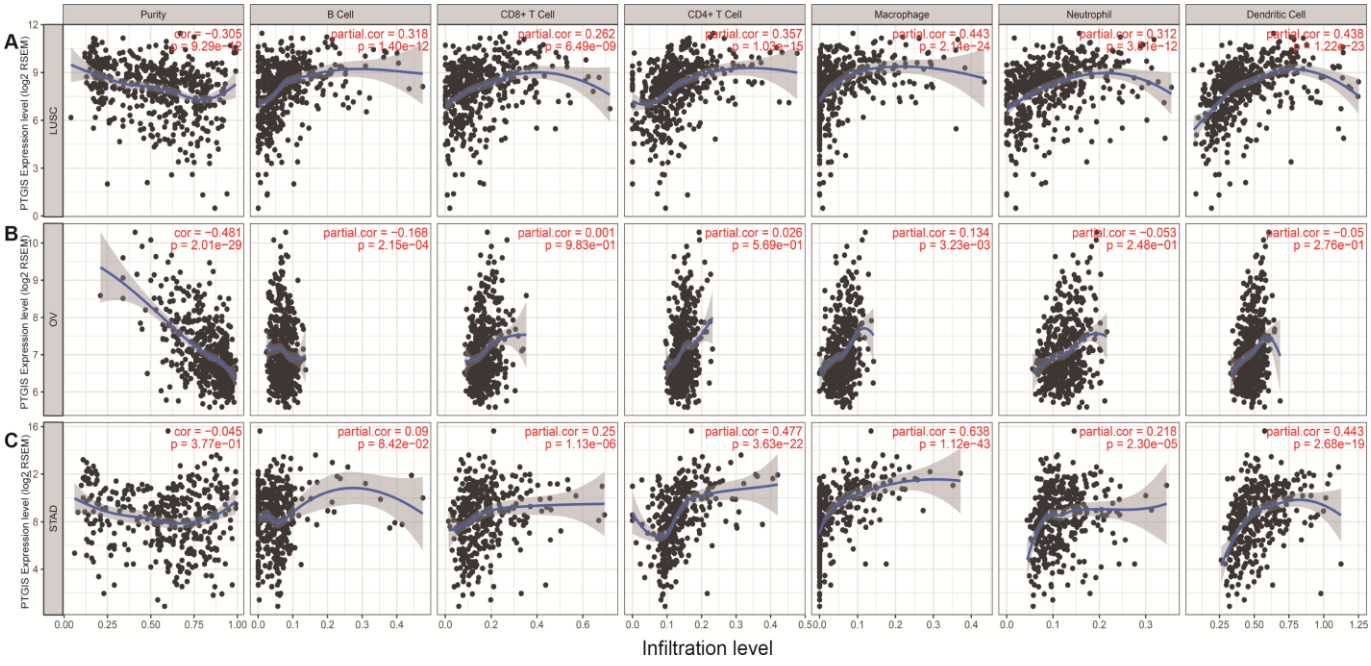

Figure 4. Correlation of PTGIS expression with immune infiltration level in LUSC (lung squamous cell carcinoma), OV (ovarian serous cystadenocarcinoma) and STAD (stomach adenocarcinoma). (**A**) PTGIS expression was significantly negatively related to tumor purity and had significant positive correlations with the levels of infiltrating B cells, CD8+ T cells, CD4+ T cells, macrophages, neutrophils, and dendritic cells in LUSC (n = 496). (**B**) PTGIS expression was significantly negatively related to tumor purity and the levels of infiltrating B cells but has no significant correlations with the levels of infiltrating CD8+ T cells, CD4+ T cells, neutrophils, and dendritic cells in OV. PTGIS expression showed a very weak positive correlation with macrophage infiltration in OV (n = 537). (**C**) PTGIS expression had no significant correlations with tumor purity and the levels of infiltrating B cells but had significant positive correlations with the levels of infiltrating CD8+ T cells, CD4+ T cells, macrophages, neutrophils, and dendritic cells in STAD (n= 407).

the correlation between PTGIS and infiltrating immune cells in the microenvironment of LUSC, OV, and STAD and indicate that PTGIS promotes significantly to the process of tumor immune escape.

DISCUSSION

PTGIS is a member of the P450 superfamily and a membrane protein that localizes to the endoplasmic reticulum. It is widely expressed in various tissues, especially in the lung, ovary, skeletal muscle and prostate. The main product of this enzyme is PGI2, which is the major metabolite of AA and a potent vasodilator and platelet aggregation inhibitor [14]. Although studies of PTGIS are still few, it is known that PTGIS may play an important role in tumorigenesis and cancer development in colon cancer, lung cancer, breast cancer, and head and neck cancer [17, 18, 34, 35]. In addition, PGI2, as a product of PTGIS, has a pro-inflammatory effect that increases microvascular permeability and an anti-inflammatory effect that stimulates T cell IL-10 production [36]. Furthermore, it was reported that PGI2 signaling could increase immature dendritic cell migration and inhibit immune responses [37]. In our study, we observed that the PTGIS expression level was associated with the prognosis of various cancers. Compared with low PTGIS expression, elevated PTGIS was associated with a poorer outcome in LUSC, OV, and STAD. Notably, high expression of PTGIS could significantly impair the prognosis of patients with lymph node metastasis in ovarian or gastric cancer. In addition, our further analysis showed that immune cell infiltration levels and various immunological markers were associated with PTGIS expression levels in LUSC, OV, and STAD. Therefore, our study provides clues to shed light on the potential effects of PTGIS in the TME and its application as a prognostic biomarker.

In our research, PTGIS mRNA expression profiles and prognosis were analyzed with datasets from multiple kinds of cancer from Oncomine and TCGA. In the comparison of various cancers with normal tissues, we observed differences in PTGIS expression. According to the analysis of the Oncomine data, PTGIS showed low expression in most tumors compared to that in normal tissues, and the TCGA data confirmed these results in BLCA, BRCA, COAD, ESCA, HNSC, KICH, KIRC, KIRP, LIHC, LUAD, LUSC, PRAD, READ, SKCM, STAD, THCA and UCEC (Figure 1A and 1B). It has been reported in the literature that hypermethylation of gene promoters leads to transcriptional silencing as a common event in cancer, and hypermethylation of the PTGIS promoter was also detected in colorectal cancer [16]. Because of the differences in data collection and processing mechanisms between different databases, the

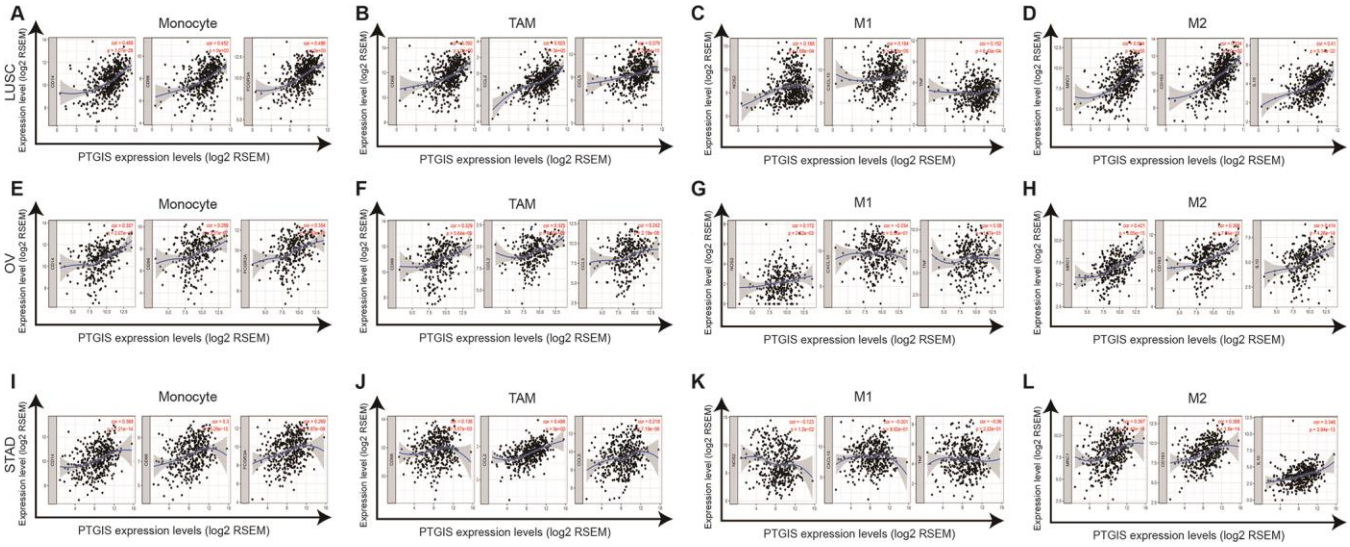

Figure 5. PTGIS expression correlated with macrophage polarization in LUSC (lung squamous cell carcinoma), OV (ovarian serous cystadenocarcinoma) and STAD (stomach adenocarcinoma). Markers included CD14, CD86 and FCGR3A for monocytes; CD68, CCL2 and CCL5 for TAMs (tumor-associated macrophages); NOS2, CXCL10, and TNF for M1 macrophages; and MRC1, CD163, and IL10 for M2 macrophages. (**A**–**D**) Scatterplots of correlation between PTGIS expression and the expression of gene markers of monocytes (A), TAMs (**B**), and M1 (**C**) and M2 macrophages (**D**) in LUSC (n = 496). (**E**–**H**) Scatterplots of correlation between PTGIS expression and the expression of gene markers of monocytes (**E**), TAMs (**F**), and M1 (**G**) and M2 macrophages (**H**) in OV (n = 537). (**I**–**L**) Scatterplots of correlation between PTGIS expression and the expression of gene markers of monocytes (**A**), TAMs (**B**), and M1 (**C**) and M2 macrophages (**D**) in STAD (n= 407).

expression of and prognosis related to PTGIS may be inconsistent in these data. For example, high expression of PTGIS was associated with a good prognosis for breast cancer patients in PrognoScan, while there was no significant effect on prognosis in Kaplan-Meier-plotter and the GEPIA database. However, in these databases, we found consistent results regarding prognosis in lung, ovarian, and gastric cancers (Figure 3 and Supplementary Figure 3). Moreover, compared with low expression of PTGIS, elevated expression of PTGIS was revealed to be associated with poorer survival outcomes for patients with stage 3 disease, patients with wild-type TP53, and patients treated with suboptimal debulking surgery in ovarian cancer, as well as for patients with advanced-stage disease or lymph node metastasis in gastric cancer. In summary, these results powerfully demonstrate that PTGIS is a prognostic marker for lung, ovarian, and gastric cancers.

We found that PTGIS expression was associated with tumor immune cell infiltration in lung, ovarian, and gastric cancers. It was reported that the types of tumor-infiltrating immune cells could be determined from statistical approaches using tumor RNA-seq data of a series of immune cell-specific genes [38]. However, tumor purity can confuse such genomic sequencing analyses, and thus, coexpression analysis should use partial correlation analysis to adjust for tumor purity [39]. After purity adjustment, we found that the correlation of genes obviously changed, especially the values in ovarian cancer, which were the most significant changes (Supplementary Tables 5 and 6). Interestingly, immune-specific genes of M1 macrophages, such as NOS2, CXCL10, and TNF, displayed weak or no correlations with PTGIS, but M2 macrophage genes, such as MRC1, CD163, and IL10, displayed relatively strong correlations (Supplementary Tables 5 and 7). These findings suggest a possible activating effect of PTGIS in the polarization of TAMs. Moreover, our other findings imply that PTGIS also influences Tregs activation and induces T cell exhaustion to some extent. Increased expression of PTGIS was positively correlated with the expression of Tregs and T cell exhaustion markers (Supplementary Table 6). These correlations may indicate a potential mechanism by which PTGIS suppresses T cell function in LUSC, OV, and STAD. Therefore, the above results show that PTGIS plays a vital role in infiltrating immune cell recruitment and functional suppression in the TME.

Previous studies have provided possible explanations for why PTGIS expression in a tumor is associated with immune infiltration and poor prognosis. Platelets are the "first responders" to cancer and metastasis, and this initial role of platelets depends on the metabolism of prostacyclins; in addition, pharmacological, clinical, and epidemiological studies indicate that nonsteroidal anti-inflammatory drugs (NSAIDs), which target cyclooxygenases, could help prevent cancer [40]. PGI2 is the primary metabolite of PTGIS, and the 5-year survival rate of lung cancer patients with high expression of PGI2 is significantly worse than that of lung cancer patients with low expression of PGI2 [41]. PGI2, as a precursor of protumorigenic metabolites, not only promotes cancer growth by activating peroxisome proliferator-activated receptor δ (PPARδ) and increases the expression levels of the proangiogenic factor vascular endothelial growth factor [42] but also seems to act primarily on TAMs, which promote all aspects of cancer growth and progression [43]. PTGIS may be a crucial factor leading to increased accumulation of PGI2 in tumors and may affect the release of inflammatory factors through the synergistic action of the AA pathway, leading to the recruitment of various immune cells in the TME. PGI2 could regulate the innate immune system, including dendritic cells, macrophages, and monocytes, by increasing anti-inflammatory IL-10 and decreasing TNF-a, IL-1a, IL-6, and IL-12 [44]. Additionally, PGI2 displays an immunosuppressive capability via elevation of cAMP levels and downregulation of NF-kB [45]. The release cytokines and growth factors into the TME are crucial for tumor progression. Thus, the interaction between the AA pathway and the TME may be a likely reason explaining why elevated PTGIS leads to poorer outcomes in LUSC, OV, and STAD.

There are some limitations in this study. Since our study is based on data from public databases, it may have biases resulting from confounding factors. Moreover, the mechanisms by which PTGIS polarizes M1 macrophages into M2 macrophages are also unclear and need to be uncovered in future studies.

Our results showed that, compared with low PTGIS, elevated PTGIS suggested worse survival outcomes and promoted immune cell infiltration in diverse tumors. In addition, in lung, ovarian, and gastric cancers, the PTGIS expression level was closely related to the activation of immune cells, especially TAMs and Tregs, as well as T cell exhaustion. Thus, PTGIS may play a role of immune suppression by affecting tumor-infiltrating immune cells and be used as a prognostic marker for lung, ovarian and gastric cancer patients.

MATERIALS AND METHODS

Oncomine database analysis

PTGIS expression levels in different tumors were analyzed via the Oncomine database (https://www.

oncomine.org) [46, 47]. The threshold settings were as follows: gene ranking of top 10%, fold change of 2.0, and P-value of 1E-4.

PrognoScan database analysis

PrognoScan (http://dna00.bio.kyutech.ac.jp/PrognoScan/) [48] is a powerful platform that contains a great number of publicly available cancer microarray datasets with corresponding clinical information and is also a tool for assessing the biological relationship between gene expression and clinical outcomes. The associations between PTGIS expression levels and different cancer patient prognoses were obtained from the PrognoScan database. The threshold was specified as a P-value < 0.05.

Kaplan-Meier-plotter database analysis

Kaplan-Meier plotter was used to analyze the association of PTGIS expression with prognosis in 5,353 breast, 3,091 ovarian, 2,909 lung, and 1,517 gastric cancer patients (http://kmplot.com/analysis/) [49]. The number of patients at risk at certain time points between subgroups based on gene expression status is provided in Kaplan-Meier survival plots. The hazard ratio (HRs), 95% confidence intervals (CIs) and log-rank P-values were calculated. A P-value <0.05 was considered statistically significant.

TIMER database analysis

Tumor Immune Estimation Resource (TIMER) is a powerful computational tool for the systematic analysis of immune cell infiltration according to RNA sequencing data from various tumors (https://cistrome.shinyapps.io/timer/) [28, 50]. The expression of PTGIS in various cancers and its correlation with the abundances of six tumor-infiltrating immune cells (TIICs) (B cells, CD4+ T cells, CD8+ T cells, macrophages, neutrophils, and dendritic cells) was analyzed by the corresponding functional modules. According to related references [51–53] and the CellMarker database (http://biocc.hrbmu.edu.cn/CellMarker/) [54], a total of 66 related gene markers of TIICs were used for the analysis. The expression scatter plots between PTGIS and immune-related gene markers based on a specific cancer type were generated by correlation modules, and Spearman's correlation coefficient and the P-value are displayed. Gene expression levels are shown as log2 RSEM values.

Gene correlation analysis in GEPIA

There is a new interactive web server for analyzing and visualizing RNA sequencing expression data called Gene Expression Profiling Interactive Analysis (GEPIA) (http://gepia.cancer-pku.cn/index.html) [29]. GEPIA is based on data from 9,736 tumors and 8,587 normal tissues from TCGA [55] and the Genotype-Tissue Expression (GTEx) Project [56], which was used to confirm the gene correlation analysis in TIMER. The survival plots of 33 different types of cancer were analyzed by GEPIA depending on the expression levels of a gene with the log-rank test. Gene expression correlation analysis was performed on tumor tissues and normal tissues using TCGA and GTEx datasets. The correlation coefficient was calculated by the Spearman method. PTGIS expression is displayed on the x-axis, and the expression of other genes is shown on the y-axis.

Statistical methods

PrognoScan and Kaplan-Meier plots were used to obtain curves related to survival outcomes, including overall survival (OS), disease-free survival (DFS), and disease-specific survival (DSS). Gene expression profiling results from Oncomine are shown with gene rankings, fold changes, and P-values. All the data were from Kaplan-Meier plotter, PrognoScan, and GEPIA, and the results are displayed with P-values based on a log-rank test and a hazard ratio (HR). Spearman's correlation coefficients and P-values were used to evaluate gene correlation. P-values less than 0.05 were considered statistically significant. The flow diagram is displayed in Supplementary Figure 1.

AUTHOR CONTRIBUTIONS

DD, BC, YF, and JL contributed to the conception and design of the study. WW, YJ, and HH contributed to data collection. DD, BC, YF, and HH analyzed and interpreted the data. DD, BC, and YF drafted the report, which was critically revised for important intellectual content by HH and JL. All authors approved the final version of the report.

CONFLICTS OF INTEREST

The authors declare no potential conflicts of interest.

FUNDING

This work was supported by the National Natural Science Foundation of China (grant number 81772782). and the High-level Hospital Construction Project (grant number DFJH201921).

REFERENCES

1. Siegel RL, Miller KD, Jemal A. Cancer statistics, 2019. CA Cancer J Clin. 2019; 69:7–34. https://doi.org/10.3322/caac.21551 PMID:30620402

2. Helmy KY, Patel SA, Nahas GR, Rameshwar P. Cancer immunotherapy: accomplishments to date and future promise. Ther Deliv. 2013; 4:1307–20. https://doi.org/10.4155/tde.13.88 PMID:24116914

3. Blank CU, Rozeman EA, Fanchi LF, Sikorska K, van de Wiel B, Kvistborg P, Krijgsman O, van den Braber M, Philips D, Broeks A, van Thienen JV, Mallo HA, Adriaansz S, et al. Neoadjuvant versus adjuvant ipilimumab plus nivolumab in macroscopic stage III melanoma. Nat Med. 2018; 24:1655–61. https://doi.org/10.1038/s41591-018-0198-0 PMID:30297911

4. Huang AC, Orlowski RJ, Xu X, Mick R, George SM, Yan PK, Manne S, Kraya AA, Wubbenhorst B, Dorfman L, D'Andrea K, Wenz BM, Liu S, et al. A single dose of neoadjuvant PD-1 blockade predicts clinical outcomes in resectable melanoma. Nat Med. 2019; 25:454–61. https://doi.org/10.1038/s41591-019-0357-y PMID:30804515

5. Forde PM, Chaft JE, Smith KN, Anagnostou V, Cottrell TR, Hellmann MD, Zahurak M, Yang SC, Jones DR, Broderick S, Battafarano RJ, Velez MJ, Rekhtman N, et al. Neoadjuvant PD-1 blockade in resectable lung cancer. N Engl J Med. 2018; 378:1976–86. https://doi.org/10.1056/NEJMoa1716078 PMID:29658848

6. Muro K, Chung HC, Shankaran V, Geva R, Catenacci D, Gupta S, Eder JP, Golan T, Le DT, Burtness B, McRee AJ, Lin CC, Pathiraja K, et al. Pembrolizumab for patients with PD-L1-positive advanced gastric cancer (KEYNOTE-012): a multicentre, open-label, phase 1b trial. Lancet Oncol. 2016; 17:717–26. https://doi.org/10.1016/S1470-2045(16)00175-3 PMID:27157491

7. Konstantinopoulos PA, Waggoner S, Vidal GA, Mita M, Moroney JW, Holloway R, Van Le L, Sachdev JC, Chapman-Davis E, Colon-Otero G, Penson RT, Matulonis UA, Kim YB, et al. Single-arm phases 1 and 2 trial of niraparib in combination with pembrolizumab in patients with recurrent platinum-resistant ovarian carcinoma. JAMA Oncol. 2019. [Epub ahead of print]. https://doi.org/10.1001/jamaoncol.2019.1048 PMID:31194228

8. Beer TM, Kwon ED, Drake CG, Fizazi K, Logothetis C, Gravis G, Ganju V, Polikoff J, Saad F, Humanski P, Piulats JM, Gonzalez Mella P, Ng SS, et al. Randomized, double-blind, phase III trial of ipilimumab versus placebo in asymptomatic or minimally symptomatic patients with metastatic chemotherapy-naive castration-resistant prostate cancer. J Clin Oncol. 2017; 35:40–47. https://doi.org/10.1200/JCO.2016.69.1584 PMID:28034081

9. Ciardiello D, Vitiello PP, Cardone C, Martini G, Troiani T, Martinelli E, Ciardiello F. Immunotherapy of colorectal cancer: challenges for therapeutic efficacy. Cancer Treat Rev. 2019; 76:22–32. https://doi.org/10.1016/j.ctrv.2019.04.003 PMID:31079031

10. Kato S, Goodman A, Walavalkar V, Barkauskas DA, Sharabi A, Kurzrock R. Hyperprogressors after immunotherapy: analysis of genomic alterations associated with accelerated growth rate. Clin Cancer Res. 2017; 23:4242–50. https://doi.org/10.1158/1078-0432.CCR-16-3133 PMID:28351930

11. Becht E, Giraldo NA, Dieu-Nosjean MC, Sautès-Fridman C, Fridman WH. Cancer immune contexture and immunotherapy. Curr Opin Immunol. 2016; 39:7–13. https://doi.org/10.1016/j.coi.2015.11.009 PMID:26708937

12. Beyrend G, van der Gracht E, Yilmaz A, van Duikeren S, Camps M, Höllt T, Vilanova A, van Unen V, Koning F, de Miranda NF, Arens R, Ossendorp F. PD-L1 blockade engages tumor-infiltrating lymphocytes to co-express targetable activating and inhibitory receptors. J Immunother Cancer. 2019; 7:217. https://doi.org/10.1186/s40425-019-0700-3 PMID:31412943

13. Hutchinson L. Immunotherapy: exploiting PD-1 on TAMs for tumour cell kill. Nat Rev Clin Oncol. 2017; 14:392–93. https://doi.org/10.1038/nrclinonc.2017.87 PMID:28607517

14. Yokoyama C, Yabuki T, Inoue H, Tone Y, Hara S, Hatae T, Nagata M, Takahashi EI, Tanabe T. Human gene encoding prostacyclin synthase (PTGIS): genomic organization, chromosomal localization, and promoter activity. Genomics. 1996; 36:296–304. https://doi.org/10.1006/geno.1996.0465 PMID:8812456

15. Ershov PV, Mezentsev YV, Kopylov AT, Yablokov EO, Svirid AV, Lushchyk AY, Kaluzhskiy LA, Gilep AA, Usanov SA, Medvedev AE, Ivanov AS. Affinity isolation and mass spectrometry identification of prostacyclin synthase (PTGIS) subinteractome. Biology (Basel). 2019; 8:49. https://doi.org/10.3390/biology8020049 PMID:31226805

16. Frigola J, Muñoz M, Clark SJ, Moreno V, Capellà G, Peinado MA. Hypermethylation of the prostacyclin synthase (PTGIS) promoter is a frequent event in colorectal cancer and associated with aneuploidy. Oncogene. 2005; 24:7320–26. https://doi.org/10.1038/sj.onc.1208883 PMID:16007128

17. Abraham JE, Harrington P, Driver KE, Tyrer J, Easton DF, Dunning AM, Pharoah PD. Common polymorphisms in the prostaglandin pathway genes and their association with breast cancer susceptibility and survival. Clin Cancer Res. 2009; 15:2181–91. https://doi.org/10.1158/1078-0432.CCR-08-0716 PMID:19276290

18. Lichao S, Liang P, Chunguang G, Fang L, Zhihua Y, Yuliang R. Overexpression of PTGIS could predict liver metastasis and is correlated with poor prognosis in colon cancer patients. Pathol Oncol Res. 2012; 18:563–69. https://doi.org/10.1007/s12253-011-9478-4 PMID:22109564

19. Zhou W, Zhang J, Goleniewska K, Dulek DE, Toki S, Newcomb DC, Cephus JY, Collins RD, Wu P, Boothby MR, Peebles RS Jr. Prostaglandin I2 suppresses proinflammatory chemokine expression, CD4 T cell activation, and STAT6-independent allergic lung inflammation. J Immunol. 2016; 197:1577–86. https://doi.org/10.4049/jimmunol.1501063 PMID:27456482

20. Liu W, Li H, Zhang X, Wen D, Yu F, Yang S, Jia X, Cong B, Ma C. Prostaglandin I2-IP signalling regulates human Th17 and treg cell differentiation. Prostaglandins Leukot Essent Fatty Acids. 2013; 89:335–44. https://doi.org/10.1016/j.plefa.2013.08.006 PMID:24035274

21. Kandukuri SR, Rao J. FIGO 2013 staging system for ovarian cancer: what is new in comparison to the 1988 staging system? Curr Opin Obstet Gynecol. 2015; 27:48–52. https://doi.org/10.1097/GCO.0000000000000135 PMID:25490382

22. Japanese Gastric Cancer Association. Japanese gastric cancer treatment guidelines 2014 (Ver. 4). Gastric Cancer. 2017; 20:1–19. https://doi.org/10.1007/s10120-016-0622-4 PMID:27342689

23. Azimi F, Scolyer RA, Rumcheva P, Moncrieff M, Murali R, McCarthy SW, Saw RP, Thompson JF. Tumor-infiltrating lymphocyte grade is an independent predictor of sentinel lymph node status and survival in patients with cutaneous melanoma. J Clin Oncol. 2012; 30:2678–83. https://doi.org/10.1200/JCO.2011.37.8539 PMID:22711850

24. Taylor RC, Patel A, Panageas KS, Busam KJ, Brady MS. Tumor-infiltrating lymphocytes predict sentinel lymph node positivity in patients with cutaneous melanoma. J Clin Oncol. 2007; 25:869–75. https://doi.org/10.1200/JCO.2006.08.9755 PMID:17327608

25. Wolf GT, Chepeha DB, Bellile E, Nguyen A, Thomas D, McHugh J, and University of Michigan Head and Neck SPORE Program. Tumor infiltrating lymphocytes (TIL) and prognosis in oral cavity squamous carcinoma: a preliminary study. Oral Oncol. 2015; 51:90–95. https://doi.org/10.1016/j.oraloncology.2014.09.006 PMID:25283344

26. Van Loo P, Nordgard SH, Lingjærde OC, Russnes HG, Rye IH, Sun W, Weigman VJ, Marynen P, Zetterberg A, Naume B, Perou CM, Børresen-Dale AL, Kristensen VN. Allele-specific copy number analysis of tumors. Proc Natl Acad Sci USA. 2010; 107:16910–15. https://doi.org/10.1073/pnas.1009843107 PMID:20837533

27. Carter SL, Cibulskis K, Helman E, McKenna A, Shen H, Zack T, Laird PW, Onofrio RC, Winckler W, Weir BA, Beroukhim R, Pellman D, Levine DA, et al. Absolute quantification of somatic DNA alterations in human cancer. Nat Biotechnol. 2012; 30:413–21. https://doi.org/10.1038/nbt.2203 PMID:22544022

28. Li T, Fan J, Wang B, Traugh N, Chen Q, Liu JS, Li B, Liu XS. TIMER: a web server for comprehensive analysis of tumor-infiltrating immune cells. Cancer Res. 2017; 77:e108–e110. https://doi.org/10.1158/0008-5472.CAN-17-0307 PMID:29092952

29. Tang Z, Li C, Kang B, Gao G, Li C, Zhang Z. GEPIA: a web server for cancer and normal gene expression profiling and interactive analyses. Nucleic Acids Res. 2017; 45:W98–W102. https://doi.org/10.1093/nar/gkx247 PMID:28407145

30. Marshall EA, Ng KW, Kung SH, Conway EM, Martinez VD, Halvorsen EC, Rowbotham DA, Vucic EA, Plumb AW, Becker-Santos DD, Enfield KS, Kennett JY, Bennewith KL, et al. Emerging roles of T helper 17 and regulatory T cells in lung cancer progression and metastasis. Mol Cancer. 2016; 15:67. https://doi.org/10.1186/s12943-016-0551-1 PMID:27784305

31. Wang X, Lang M, Zhao T, Feng X, Zheng C, Huang C, Hao J, Dong J, Luo L, Li X, Lan C, Yu W, Yu M, et al. cancer-FOXP3 directly activated CCL5 to recruit FOXP3^{+} treg cells in pancreatic ductal adenocarcinoma. Oncogene. 2017; 36:3048–58. https://doi.org/10.1038/onc.2016.458 PMID:27991933

32. Sakuishi K, Apetoh L, Sullivan JM, Blazar BR, Kuchroo VK, Anderson AC. Targeting tim-3 and PD-1 pathways to reverse T cell exhaustion and restore anti-tumor immunity. J Exp Med. 2010; 207:2187–94. https://doi.org/10.1084/jem.20100643 PMID:20819927

33. Monney L, Sabatos CA, Gaglia JL, Ryu A, Waldner H, Chernova T, Manning S, Greenfield EA, Coyle AJ, Sobel RA, Freeman GJ, Kuchroo VK. Th1-specific cell surface protein tim-3 regulates macrophage activation and severity of an autoimmune disease. Nature. 2002; 415:536–41. https://doi.org/10.1038/415536a PMID:11823861

34. Cathcart MC, Al-Sarraf N, Boyle E, O'Byrne KJ, Pidgeon GP, Gray SG. 66 Prostacyclin synthase (PTGIS): expression and epigenetic regulation in lung cancer. Lung Cancer. 2007; 57:S18. https://doi.org/10.1016/S0169-5002(07)70392-6

35. Lee WT, Huang CC, Chen KC, Wong TY, Ou CY, Tsai ST, Yen CJ, Fang SY, Lo HI, Wu YH, Hsueh WT, Yang MW, Lin FC, et al. Genetic polymorphisms in the prostaglandin pathway genes and risk of head and neck cancer. Oral Dis. 2015; 21:207–15. https://doi.org/10.1111/odi.12244 PMID:24724948

36. Takahashi Y, Tokuoka S, Masuda T, Hirano Y, Nagao M, Tanaka H, Inagaki N, Narumiya S, Nagai H. Augmentation of allergic inflammation in prostanoid IP receptor deficient mice. Br J Pharmacol. 2002; 137:315–22. https://doi.org/10.1038/sj.bjp.0704872 PMID:12237250

37. Toki S, Goleniewska K, Huckabee MM, Zhou W, Newcomb DC, Fitzgerald GA, Lawson WE, Peebles RS Jr. PGI_2 signaling inhibits antigen uptake and increases migration of immature dendritic cells. J Leukoc Biol. 2013; 94:77–88. https://doi.org/10.1189/jlb.1112559 PMID:23625201

38. Finotello F, Trajanoski Z. Quantifying tumor-infiltrating immune cells from transcriptomics data. Cancer Immunol Immunother. 2018; 67:1031–40. https://doi.org/10.1007/s00262-018-2150-z PMID:29541787

39. Aran D, Sirota M, Butte AJ. Systematic pan-cancer analysis of tumour purity. Nat Commun. 2015; 6:8971. https://doi.org/10.1038/ncomms9971 PMID:26634437

40. Kanikarla-Marie P, Kopetz S, Hawk ET, Millward SW, Sood AK, Gresele P, Overman M, Honn K, Menter DG. Bioactive lipid metabolism in platelet "first responder" and cancer biology. Cancer Metastasis Rev. 2018; 37:439–54. https://doi.org/10.1007/s10555-018-9755-8 PMID:30112590

41. Xin C, Chu L, Zhang L, Geng D, Wang Y, Sun D, Sui P, Zhao X, Gong Z, Sui M, Zhang W. Expression of cytosolic phospholipase A2 (cPLA2)-arachidonic acid (AA)-cyclooxygenase-2 (COX-2) pathway factors in lung cancer patients and its implication in lung cancer early detection and prognosis. Med Sci Monit. 2019; 25:5543–51. https://doi.org/10.12659/MSM.915314 PMID:31347609

42. Wang J, Ikeda R, Che XF, Ooyama A, Yamamoto M, Furukawa T, Hasui K, Zheng CL, Tajitsu Y, Oka T, Tabata S, Nishizawa Y, Eizuru Y, Akiyama S. VEGF expression is augmented by hypoxia-induced PGIS in human fibroblasts. Int J Oncol. 2013; 43:746–54. https://doi.org/10.3892/ijo.2013.1994 PMID:23807031

43. Reinartz S, Finkernagel F, Adhikary T, Rohnalter V, Schumann T, Schober Y, Nockher WA, Nist A, Stiewe T, Jansen JM, Wagner U, Müller-Brüsselbach S, Müller R. A transcriptome-based global map of signaling pathways in the ovarian cancer microenvironment associated with clinical outcome. Genome Biol. 2016; 17:108. https://doi.org/10.1186/s13059-016-0956-6 PMID:27215396

44. Dorris SL, Peebles RS Jr. PGI2 as a regulator of inflammatory diseases. Mediators Inflamm. 2012; 2012:926968. https://doi.org/10.1155/2012/926968 PMID:22851816

45. Zhou W, Blackwell TS, Goleniewska K, O'Neal JF, Fitzgerald GA, Lucitt M, Breyer RM, Peebles RS Jr. Prostaglandin I2 analogs inhibit Th1 and Th2 effector cytokine production by CD4 T cells. J Leukoc Biol. 2007; 81:809–17. https://doi.org/10.1189/jlb.0606375 PMID:17135575

46. Rhodes DR, Yu J, Shanker K, Deshpande N, Varambally R, Ghosh D, Barrette T, Pandey A, Chinnaiyan AM. ONCOMINE: a cancer microarray database and integrated data-mining platform. Neoplasia. 2004; 6:1–6. https://doi.org/10.1016/s1476-5586(04)80047-2 PMID:15068665

47. Rhodes DR, Kalyana-Sundaram S, Mahavisno V, Varambally R, Yu J, Briggs BB, Barrette TR, Anstet MJ, Kincead-Beal C, Kulkarni P, Varambally S, Ghosh D, Chinnaiyan AM. Oncomine 3.0: genes, pathways, and networks in a collection of 18,000 cancer gene expression profiles. Neoplasia. 2007; 9:166–80. https://doi.org/10.1593/neo.07112 PMID:17356713

48. Mizuno H, Kitada K, Nakai K, Sarai A. PrognoScan: a new database for meta-analysis of the prognostic value of genes. BMC Med Genomics. 2009; 2:18.

https://doi.org/10.1186/1755-8794-2-18
PMID:19393097

49. Győrffy B, Lanczky A, Eklund AC, Denkert C, Budczies J, Li Q, Szallasi Z. An online survival analysis tool to rapidly assess the effect of 22,277 genes on breast cancer prognosis using microarray data of 1,809 patients. Breast Cancer Res Treat. 2010; 123:725–31. https://doi.org/10.1007/s10549-009-0674-9 PMID:20020197

50. Li B, Severson E, Pignon JC, Zhao H, Li T, Novak J, Jiang P, Shen H, Aster JC, Rodig S, Signoretti S, Liu JS, Liu XS. Comprehensive analyses of tumor immunity: implications for cancer immunotherapy. Genome Biol. 2016; 17:174. https://doi.org/10.1186/s13059-016-1028-7 PMID:27549193

51. Danaher P, Warren S, Dennis L, D'Amico L, White A, Disis ML, Geller MA, Odunsi K, Beechem J, Fling SP. Gene expression markers of tumor infiltrating leukocytes. J Immunother Cancer. 2017; 5:18. https://doi.org/10.1186/s40425-017-0215-8 PMID:28239471

52. Denda-Nagai K, Irimura T. MGL/CD301 as a unique C-type lectin expressed on dendritic cells and macrophages. In: Yamasaki S, ed. C-type lectin receptors in immunity. (Tokyo: Springer, 2016). https://doi.org/10.1007/978-4-431-56015-9_11

53. Zhang C, Yu X, Gao L, Zhao Y, Lai J, Lu D, Bao R, Jia B, Zhong L, Wang F, Liu Z. Noninvasive imaging of CD206-positive M2 macrophages as an early biomarker for post-chemotherapy tumor relapse and lymph node metastasis. Theranostics. 2017; 7:4276–88. https://doi.org/10.7150/thno.20999 PMID:29158825

54. Zhang X, Lan Y, Xu J, Quan F, Zhao E, Deng C, Luo T, Xu L, Liao G, Yan M, Ping Y, Li F, Shi A, et al. CellMarker: a manually curated resource of cell markers in human and mouse. Nucleic Acids Res. 2019; 47:D721–D728. https://doi.org/10.1093/nar/gky900 PMID:30289549

55. Tomczak K, Czerwińska P, Wiznerowicz M. The cancer genome atlas (TCGA): an immeasurable source of knowledge. Contemp Oncol (Pozn). 2015; 19:A68–77. https://doi.org/10.5114/wo.2014.47136 PMID:25691825

56. GTEx Consortium. The Genotype-Tissue Expression (GTEx) project. Nat Genet. 2013; 45:580–5. https://doi.org/10.1038/ng.2653 PMID:23715323

SUPPLEMENTARY MATERIALS

Supplementary Figures

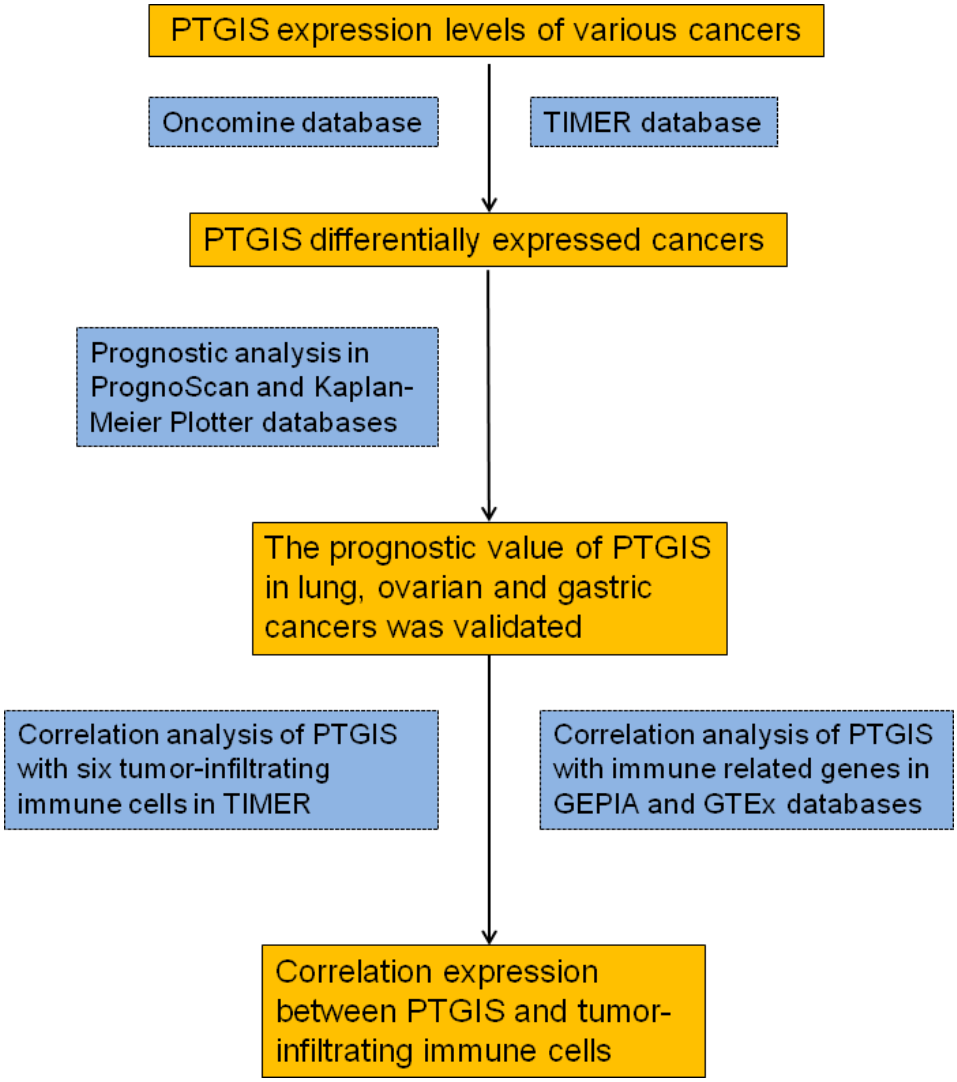

Supplementary Figure 1. Flow diagram.

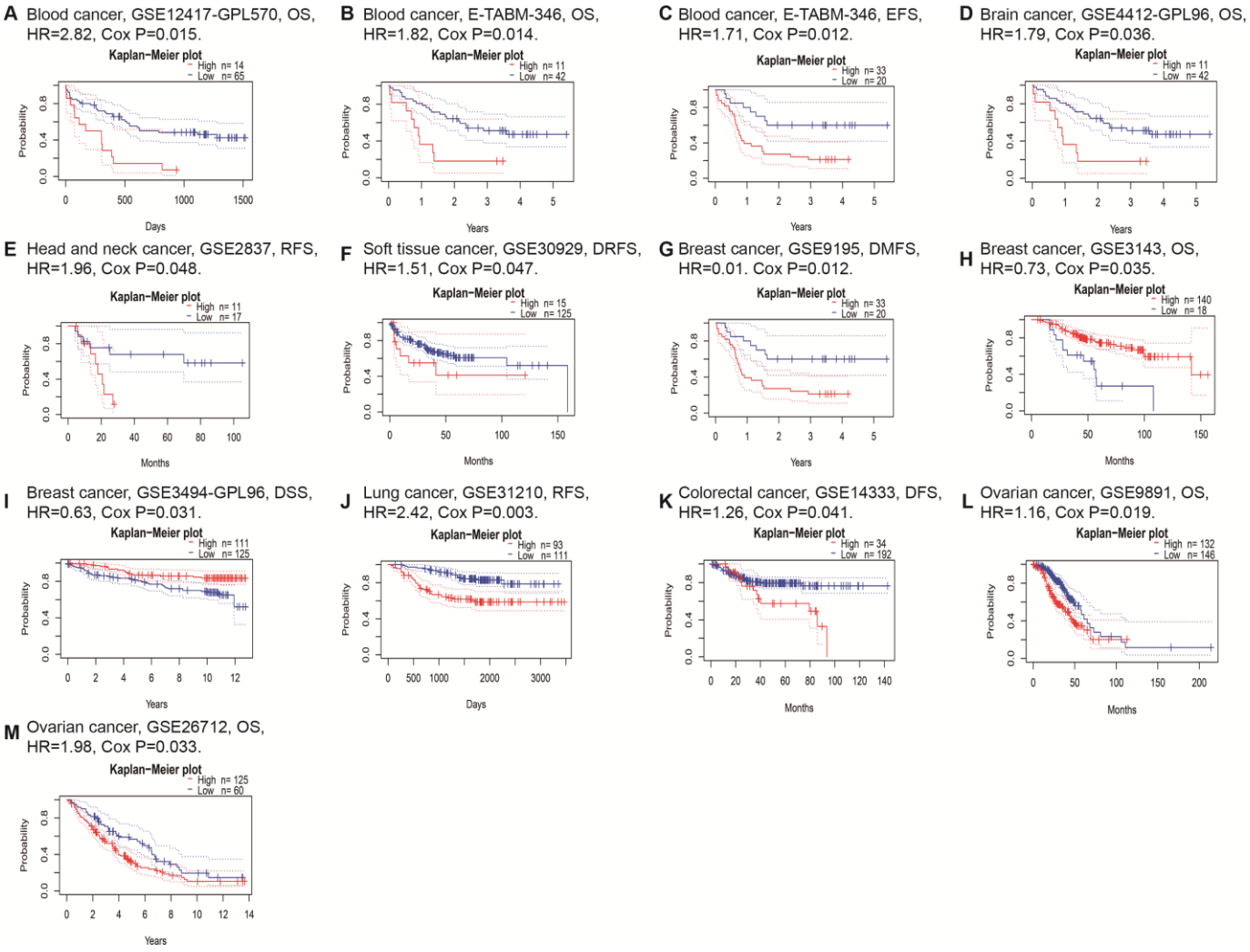

Supplementary Figure 2. Survival curves of high or low expression of PTGIS in different tumors from the PrognoScan database.

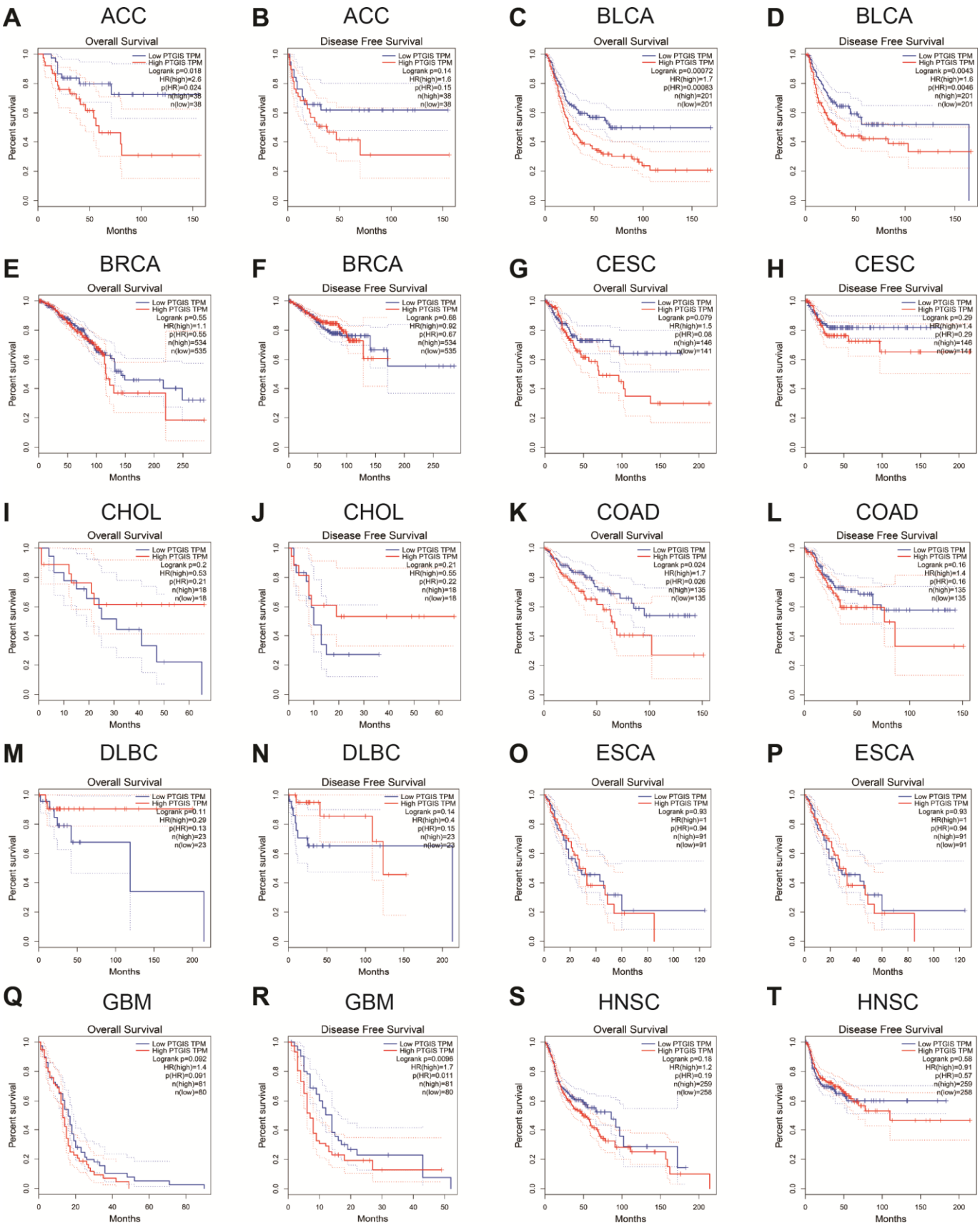
A
ACC
Overall Survival
B
ACC
Disease Free Survival
C
BLCA
Overall Survival
D
BLCA
Disease Free Survival
E
BRCA
Overall Survival
F
BRCA
Disease Free Survival
G
CESC
Overall Survival
H
CESC
Disease Free Survival
I
CHOL
Overall Survival
J
CHOL
Disease Free Survival
K
COAD
Overall Survival
L
COAD
Disease Free Survival
M
DLBC
Overall Survival
N
DLBC
Disease Free Survival
O
ESCA
Overall Survival
P
ESCA
Overall Survival
Q
GBM
Overall Survival
R
GBM
Disease Free Survival
S
HNSC
Overall Survival
T
HNSC
Disease Free Survival
Low PTGIS TPM
High PTGIS TPM
Percent survival
Months

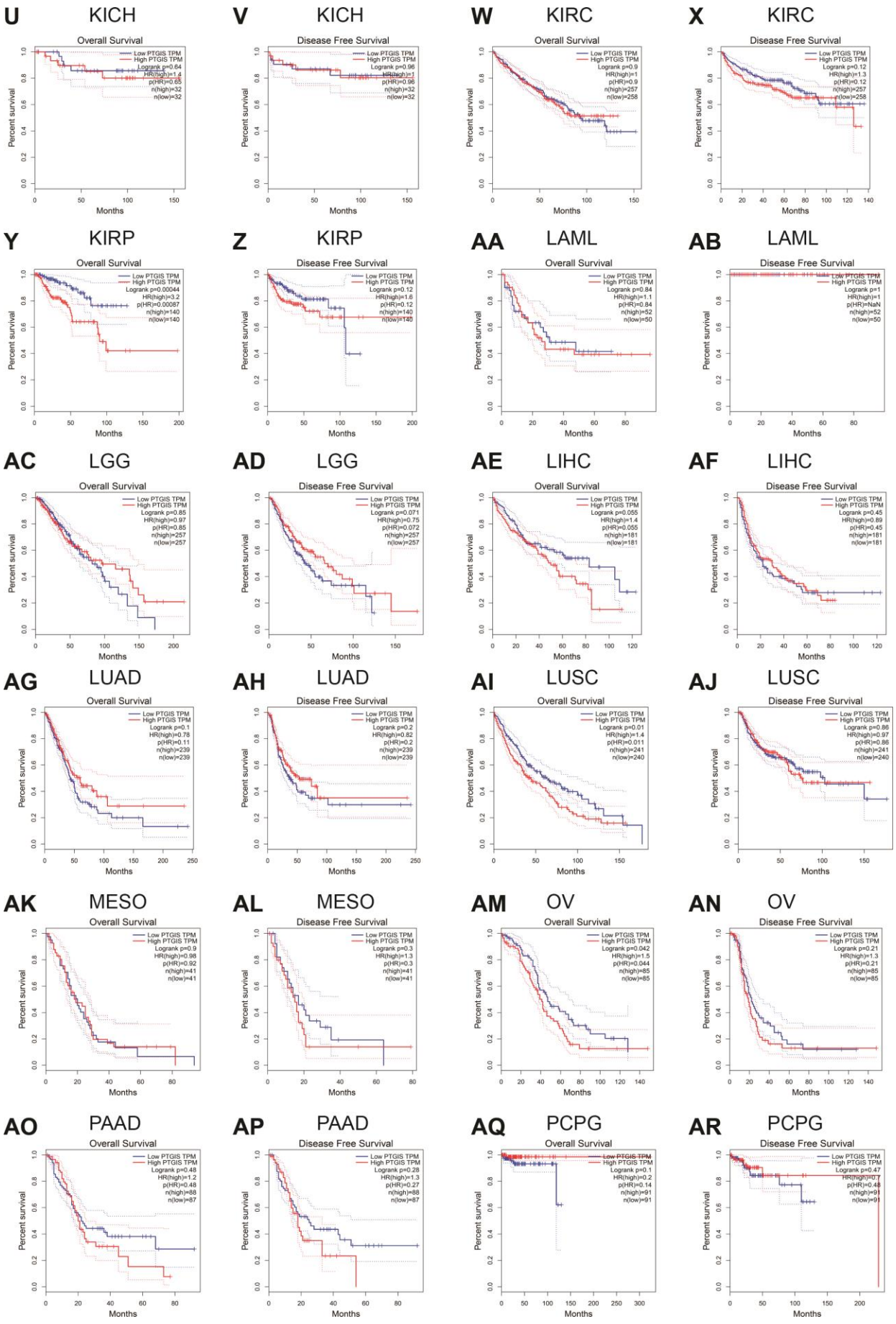
U KICH
Overall Survival
V KICH
Disease Free Survival
W KIRC
Overall Survival
X KIRC
Disease Free Survival
Y KIRP
Overall Survival
Z KIRP
Disease Free Survival
AA LAML
Overall Survival
AB LAML
Disease Free Survival
AC LGG
Overall Survival
AD LGG
Disease Free Survival
AE LIHC
Overall Survival
AF LIHC
Disease Free Survival
AG LUAD
Overall Survival
AH LUAD
Disease Free Survival
AI LUSC
Overall Survival
AJ LUSC
Disease Free Survival
AK MESO
Overall Survival
AL MESO
Disease Free Survival
AM OV
Overall Survival
AN OV
Disease Free Survival
AO PAAD
Overall Survival
AP PAAD
Disease Free Survival
AQ PCPG
Overall Survival
AR PCPG
Disease Free Survival
Low PTGIS TPM
High PTGIS TPM
Percent survival
Months

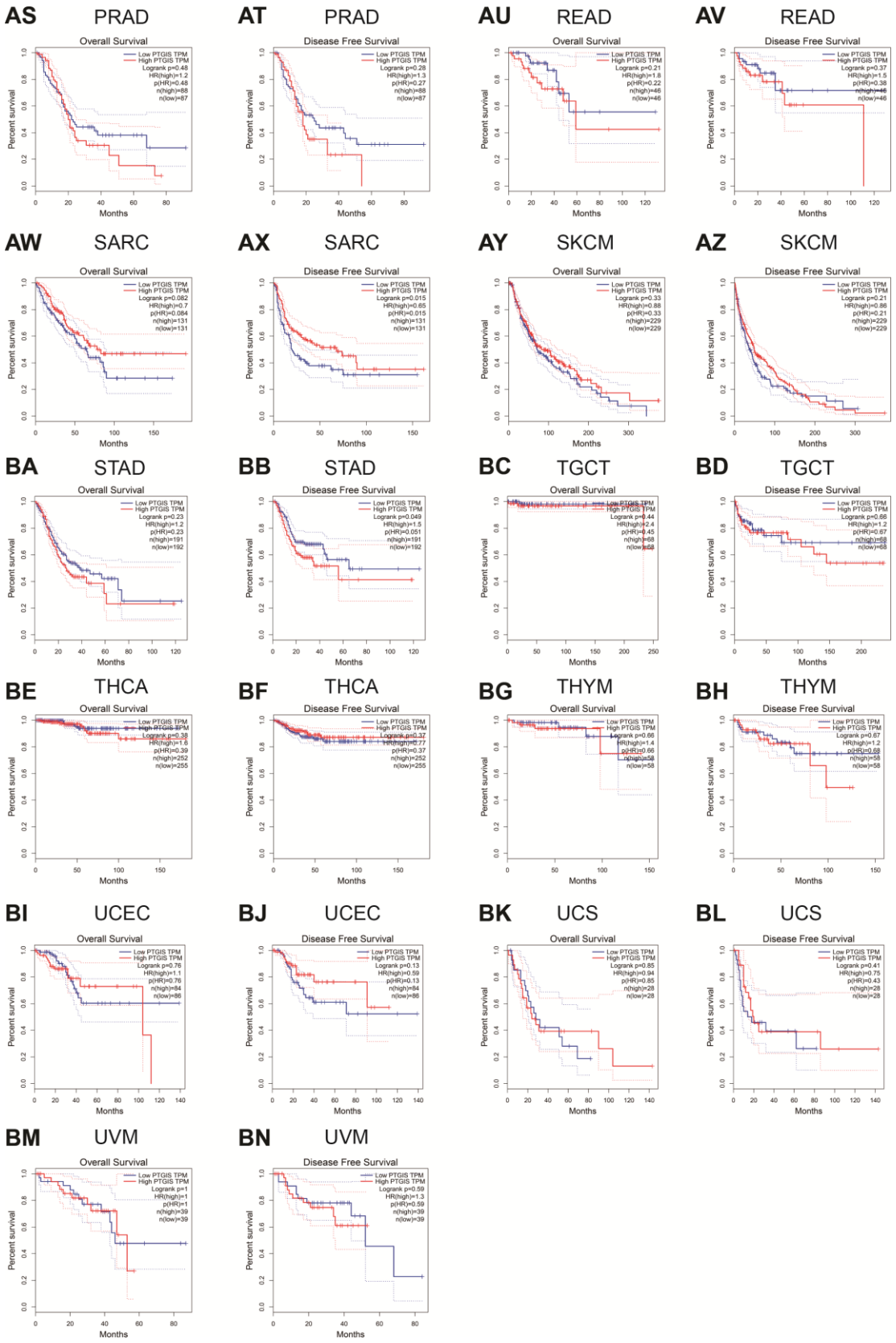

Supplementary Figure 3. Correlation of PTGIS expression with prognosis in diverse types of cancer.

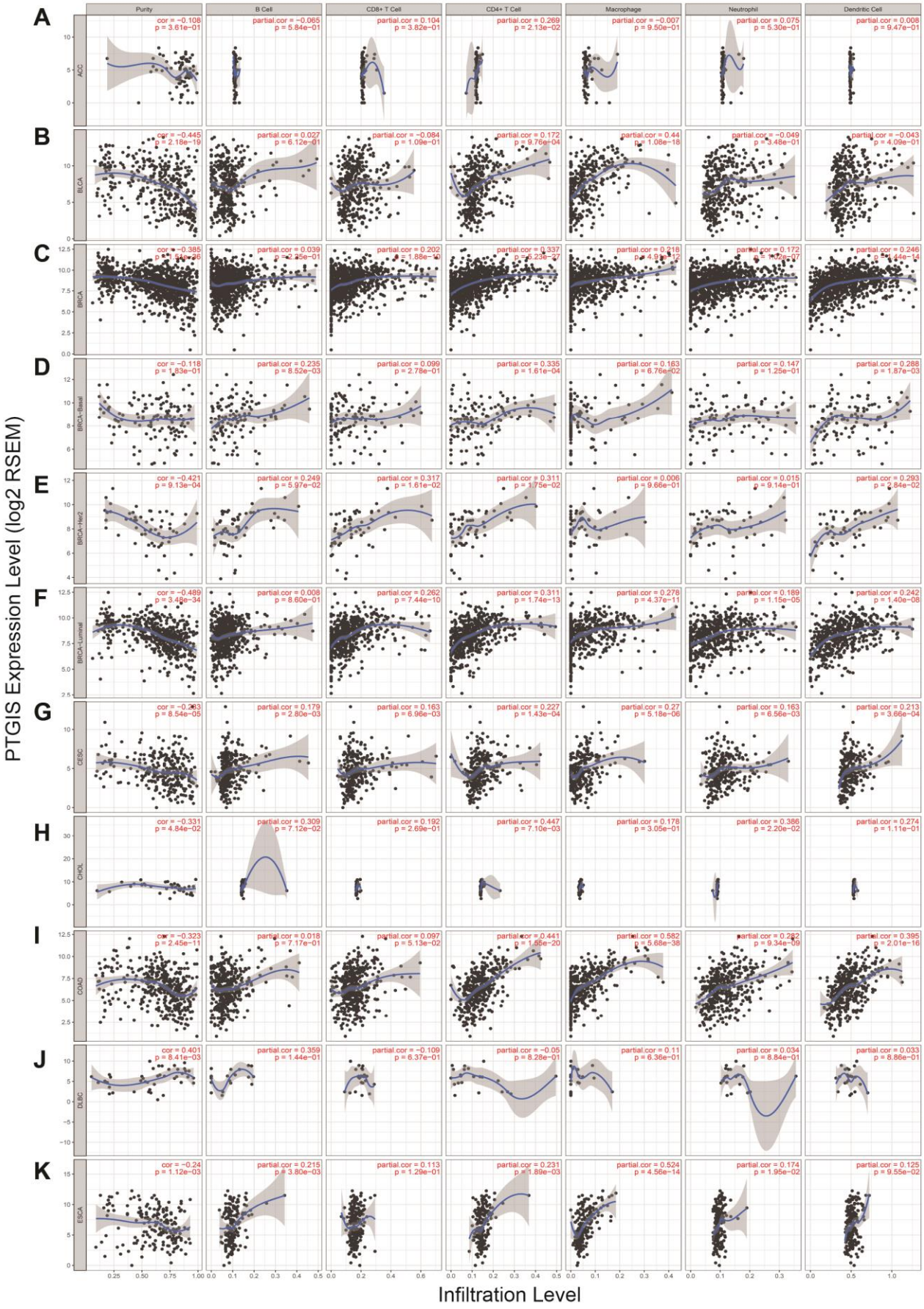
Purity
B Cell
CD8+ T Cell
CD4+ T Cell
Macrophage
Neutrophil
Dendritic Cell
A
ACC
B
BLCA
C
BRCA
D
BRCA-Basal
E
BRCA-Her2
F
BRCA-Luminal
G
CESC
H
CHOL
I
COAD
J
DLBC
K
ESCA
PTGIS Expression Level (log2 RSEM)
Infiltration Level

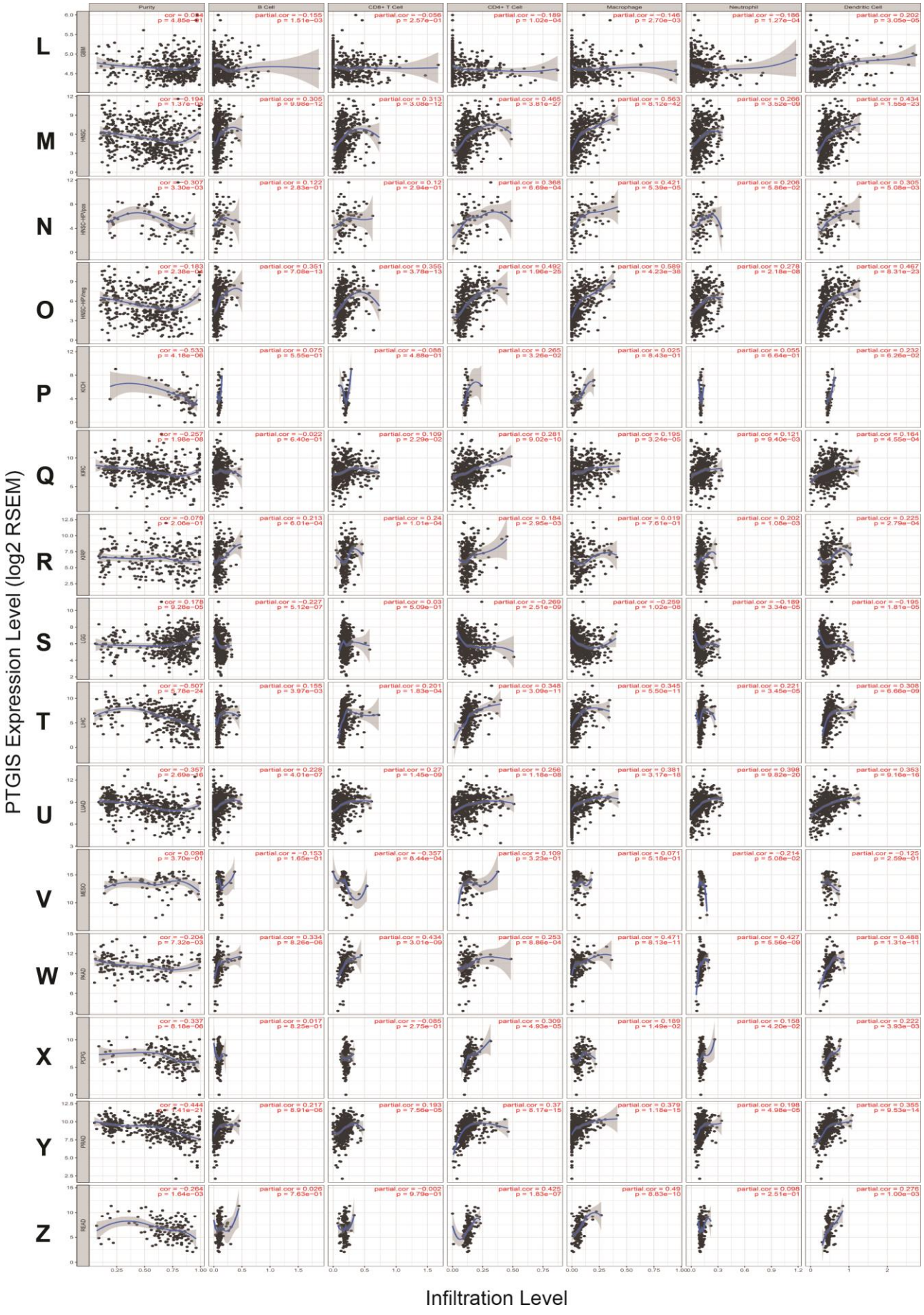
PTGIS Expression Level (log2 RSEM)
Infiltration Level
Purity
B Cell
CD8+ T Cell
CD4+ T Cell
Macrophage
Neutrophil
Dendritic Cell
GBM
HNSC
HNSC-HPVpos
HNSC-HPVneg
KICH
KIRC
KIRP
LGG
LIHC
LUAD
MESO
PAAD
PCPG
PRAD
READ
L
M
N
O
P
Q
R
S
T
U
V
W
X
Y
Z

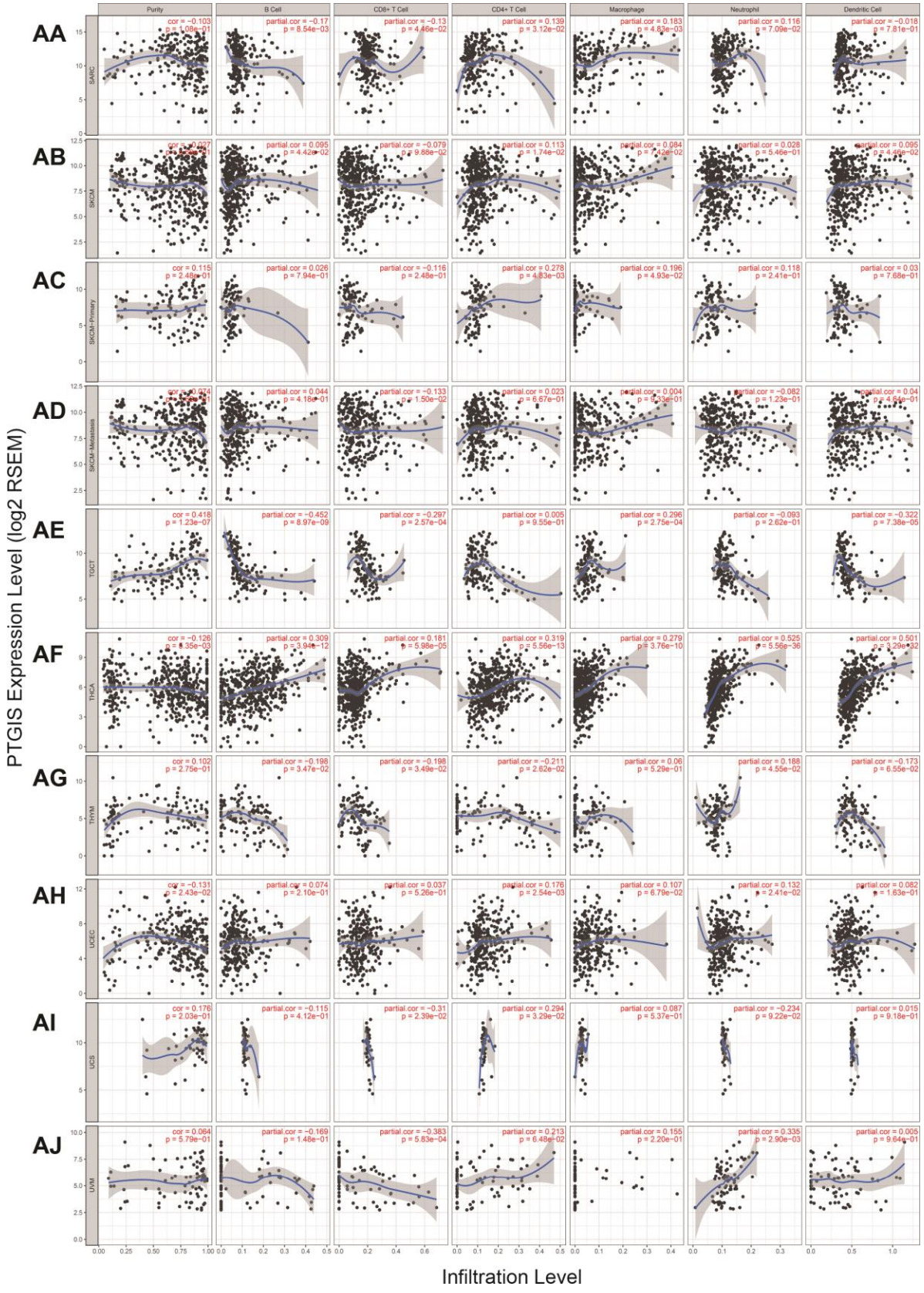

Supplementary Figure 4. Correlation of PTGIS expression with tumor-infiltrating immune cells in various types of cancers via the TIMER database.

Supplementary Tables

Supplementary Table 1. PTGIS expression in cancers vs. normal tissue in Oncomine database.

Cancer	Cancer type	P-value	Fold change	Rank (%)	Sample	Reference (PMID)
Bladder	Superficial Bladder Cancer	8.01E-25	-31.339	1%	76	16432078
	Infiltrating Bladder Urothelial Carcinoma	7.30E-24	-8.600	1%	129	16432078
	Superficial Bladder Cancer	1.28E-15	-4.420	1%	194	20421545
	Infiltrating Bladder Urothelial Carcinoma	2.09E-07	-2.889	4%	130	20421545
	Superficial Bladder Cancer	7.13E-07	-3.141	4%	42	15173019
Breast	Invasive Breast Carcinoma Stroma	6.26E-14	6.187	7%	59	18438415
	Ductal Breast Carcinoma	1.39E-07	-2.352	1%	39	10963602
	Invasive Breast Carcinoma	1.88E-08	-3.227	4%	165	22522925
	Invasive Ductal and Invasive Lobular Breast Carcinoma	6.68E-30	-2.667	4%	234	22522925
	Invasive Lobular Breast Carcinoma	2.97E-29	-2.341	5%	292	22522925
	Medullary Breast Carcinoma	9.26E-12	-2.592	6%	176	22522925
	Invasive Ductal Breast Carcinoma	1.20E-47	-2.943	6%	1700	22522925
	Tubular Breast Carcinoma	1.25E-18	-2.339	8%	211	22522925
	Mucinous Breast Carcinoma	7.35E-13	-3.019	9%	190	22522925
	Invasive Ductal Breast Carcinoma	2.96E-21	-5.071	9%	450	TCGA
Cervical	Cervical Squamous Cell Carcinoma	1.55E-06	-2.400	4%	56	18506748
	Cervical Squamous Cell Carcinoma	1.23E-06	-3.521	3%	45	18191186
Colorectal	Cecum Adenocarcinoma	3.87E-10	-7.035	8%	44	TCGA
	Rectal Adenocarcinoma	9.26E-13	-7.478	10%	82	TCGA
Head and Neck	Tongue Squamous Cell Carcinoma	9.85E-07	-5.788	3%	57	19138406
Kidney	Papillary Renal Cell Carcinoma	5.43E-18	4.434	1%	34	16115910
	Renal Oncocytoma	2.65E-18	2.870	2%	35	16115910
	Chromophobe Renal Cell Carcinoma	3.86E-06	2.892	5%	29	16115910
	Clear Cell Sarcoma of the Kidney	1.45E-07	-13.915	1%	17	16299227
Leukemia	Chronic Lymphocytic Leukemia	6.88E-05	-2.242	6%	111	15459216
Liver	Cirrhosis	8.49E-13	2.758	5%	77	19098997
	Hepatocellular Carcinoma	5.22E-20	-3.308	2%	171	12058060
	Hepatocellular Carcinoma	2.84E-46	-2.562	3%	445	21159642
	Hepatocellular Carcinoma	2.91E-06	-2.407	6%	43	21159642
Lung	Lung Adenocarcinoma	2.73E-08	-2.500	3%	39	16314486
	Lung Carcinoid Tumor	1.06E-07	-58.003	6%	37	11707567
	Lung Adenocarcinoma	2.60E-17	-2.314	4%	116	22613842
	Lung Adenocarcinoma	6.11E-06	-2.780	8%	57	17540040
Melanoma	Cutaneous Melanoma	9.44E-05	2.148	1%	18	18442402
	Benign Melanocytic Skin Nevus	2.05E-06	-5.545	2%	25	16243793
	Cutaneous Melanoma	7.38E-09	-11.640	3%	52	16243793
Ovarian	Ovarian Serous Cystadenocarcinoma	3.00E-06	-6.836	3%	594	TCGA
	Ovarian Carcinoma	3.74E-07	-6.303	8%	195	18593951
	Ovarian Serous Adenocarcinoma	7.59E-07	-4.999	10%	45	19486012
Pancreatic	Pancreatic Ductal Adenocarcinoma	9.45E-05	2.826	1%	49	16053509
	Pancreatic Ductal Adenocarcinoma	3.20E-11	4.660	3%	78	19260470
Prostate	Prostate Carcinoma	6.69E-07	-2.467	5%	87	22722839
Sarcoma	Gastrointestinal Stromal Tumor	2.23E-13	9.876	1%	25	21447720
	Clear Cell Sarcoma of the Kidney	1.45E-07	-13.915	1%	17	16299227
Other	Pleural Malignant Mesothelioma	1.33E-06	3.368	2%	49	15920167
	Teratoma	1.05E-07	3.328	5%	20	16424014

Supplementary Table 2. Positive results associated with PTGIS expression in different cancers from Prognoscan database.

Cancer type	Dataset	Endpoint	N	Hazard ratio (95%CI)	Cox P-value
Blood cancer	GSE12417-GPL570	OS	79	2.82 [1.23 - 6.47]	0.015
	E-TABM-346	EFS	53	1.71 [1.12 - 2.59]	0.012
	E-TABM-346	OS	53	1.82 [1.13 - 2.94]	0.014
Brain cancer	GSE4412-GPL96	OS	74	1.79 [1.04 - 3.09]	0.036
Breast cancer	GSE3143	OS	158	0.73 [0.55 - 0.98]	0.035
	GSE9195	DMFS	77	0.01 [0.00 - 0.39]	0.012
	GSE1456-GPL96	DSS	159	0.60 [0.40 - 0.90]	0.013
	GSE1456-GPL96	OS	159	0.63 [0.44 - 0.90]	0.012
	GSE3494-GPL96	DSS	236	0.63 [0.42 - 0.96]	0.031
Colorectal cancer	GSE17536	DSS	177	1.34 [1.01 - 1.77]	0.042
	GSE17536	DFS	145	1.63 [1.15 - 2.30]	0.006
	GSE14333	DFS	226	1.26 [1.01 - 1.58]	0.041
Head and neck cancer	GSE2837	RFS	28	1.96 [1.01 - 3.83]	0.048
Lung cancer	GSE31210	RFS	204	2.42 [1.35 - 4.35]	0.003
	GSE14814	OS	90	7.50 [1.68 - 33.39]	0.008
	GSE14814	DFS	90	5.88 [1.05 - 33.10]	0.044
Ovarian cancer	GSE9891	OS	278	1.16 [1.02 - 1.32]	0.019
	GSE8841	OS	81	4.00 [1.29 - 12.42]	0.016
	GSE26712	DFS	185	1.90 [1.06 - 3.40]	0.031
	GSE26712	OS	185	1.98 [1.06 - 3.70]	0.033
Soft tissue cancer	GSE30929	DRFS	140	1.51 [1.00 - 2.28]	0.047

Abbreviation: OS Overall survival; DFS Disease free survival; EFS Event free survival; DMFS Distant metastasis free survival; RFS Relapse free survival; DSS Disease specific survival; CI Confidence interval

Supplementary Table 3. Correlation of PTGIS mRNA expression and clinicopathological factors in ovarian cancer by Kaplan-Meier plotter database.

Variables of ovarian cancer	Overall survival (n=1657)			Progression-free survival (n=1436)		
	N	Hazard ratio	P-value	N	Hazard ratio	P-value
Histology						
Endometroid	37	2.84(0.47-17.01)	0.2319	51	2.15(0.71-6.55)	0.1677
Serous	1207	1.26(1.07-1.48)	**0.0055**	1104	1.33(1.14-1.54)	**0.0002**
Stage						
1	74	3.39(0.74-15.51)	0.0940	96	2.48(0.69-8.91)	0.1498
2	61	2.39(0.51-11.23)	0.2574	67	2.34(0.9-6.09)	0.0721
3	1044	1.2(1.01-1.42)	**0.0398**	919	1.28(1.09-1.50)	**0.0025**
4	176	1.39(0.92-2.11)	0.1159	162	0.82(0.54-1.24)	0.3466
Grade						
1	56	2.44(0.9-6.59)	0.0698	37	4.93(1.61-15.08)	0.0020
2	324	1.41(1.03-1.92)	**0.0305**	256	1.96(1.41-2.72)	**4.60E-05**
3	1015	1.16(0.97-1.38)	0.0940	837	1.24(1.05-1.48)	0.0123
TP53 mutation						
Mutated	506	1.27(0.98-1.65)	0.0651	483	1.27(0.98-1.63)	0.0663
Wild type	94	2.2(1.27-3.8)	**0.0040**	84	1.57(0.87-2.83)	0.1291
Debulk						
Optimal	801	1.21(0.99-1.49)	0.0656	696	1.26(1.04-1.53)	**0.0181**
Suboptimal	536	1.26(1.03-1.54)	**0.0266**	459	0.80(0.65-0.99)	**0.0375**
Chemotherapy						
contains platin	1409	1.29(1.12-1.49)	**0.0003**	1259	1.23(1.08-1.40)	**0.0017**
contains Taxol	793	1.24(1.01-1.52)	**0.0369**	715	1.28(1.08-1.52)	**0.0041**
contains Taxol+platin	776	1.24(1.01-1.53)	**0.0404**	698	1.28(1.08-1.53)	**0.0049**
contains Avastin	50	2.08(0.72-6.02)	0.1693	50	1.75(0.83-3.70)	0.1390

contains Docetaxel	108	1.46(0.8-2.64)	0.2129	106	1.96(1.13-3.39)	**0.0141**
contains Gemcitabine	135	1.64(1.07-2.52)	**0.0230**	131	1.49(0.95-2.34)	0.0787
contains Paclitaxel	220	1.53(0.97-2.42)	0.0658	229	1.32(0.92-1.90)	0.1346
contains Topotecan	119	1.66(1.11-2.49)	**0.0133**	118	1.41(0.90-2.20)	0.1307

Bold values indicate P < 0.05.

Supplementary Table 4. Correlation of PTGIS mRNA expression and clinicopathological factors in gastric cancer by Kaplan-Meier plotter database.

Variables of gastric cancer	Overall survival		(n=882)	Progression-free survival		(n=646)
	N	Hazard ratio	P-value	N	Hazard ratio	P-value
Gender						
Female	236	1.13(0.98-1.31)	0.1003	201	2.07(1.40-3.04)	**0.0002**
Male	545	2.18(1.75-2.70)	**5.80E-13**	438	2.20(1.73-2.80)	**4.70E-11**
Stage						
2	140	2.17(1.17-4.02)	**0.0118**	131	1.58(0.84-2.95)	0.1499
3	305	2.39(1.63-3.50)	**4.00E-06**	186	1.84(1.25-2.69)	**0.0015**
4	148	1.48(1.00-2.20)	**0.0485**	141	1.38(0.93-2.04)	0.1114
Stage T						
2	241	1.60(1.03-2.50)	**0.0358**	239	1.51(1.00-2.29)	**0.0495**
3	204	2.48(1.63-3.77)	**1.30E-05**	204	1.81(1.23-2.67)	**0.0024**
4	38	1.82(0.72-4.62)	**0.1992**	39	2.13(0.95-4.76)	0.0605
Stage N						
0	74	2.43(0.99-5.93)	**0.0453**	72	2.10(0.88-5.01)	0.0868
1	225	2.19(1.44-3.32)	**0.0002**	222	2.00(1.35-2.97)	**0.0005**
2	121	3.12(1.95-4.98)	**5.60E-07**	125	2.33(1.50-3.61)	**1.00E-04**
3	76	1.70(0.99-2.94)	0.0538	76	1.75(1.01-3.02)	**0.0428**
1+2+3	422	2.08(1.57-2.74)	**1.50E-07**	423	1.76(1.37-2.28)	**1.10E-05**
Stage M						
0	444	2.03(1.51-2.72)	**1.80E-06**	443	1.64(1.26-2.14)	**0.0002**
1	56	1.87(1.03-3.41)	**0.0372**	56	0.70(0.36-1.34)	0.2771
HER2 status						
negative	532	2.06(1.62-2.62)	**1.50E-09**	408	1.88(1.44-2.45)	**2.00E-06**
positive	344	1.98(1.50-2.61)	**7.30E-07**	233	2.43(1.76-3.37)	**3.20E-08**
Lauren classification						
Intestinal	320	2.33(1.70-3.21)	**8.10E-08**	263	1.81(1.27-2.57)	**0.0009**
Diffuse	241	1.75(1.22-2.52)	**0.0022**	231	1.54(1.09-2.17)	**0.0134**
Differentiation						
poorly	165	0.76(0.48-1.20)	0.2404	121	0.66(0.38-1.12)	0.1192
moderately	67	3.56(1.22-10.43)	**0.0145**	67	3.10(1.18-8.15)	**0.0167**

Bold values indicate P < 0.05.

Supplementary Table 5. Correlation analysis between PTGIS and relate genes and markers of innate immunity cells in TIMER.

Description	Gene markers	LUSC				OV				STAD			
		Purity		None		Purity		None		Purity		None	
		Cor	P	Cor	P	Cor	P	Cor	P	Cor	P	Cor	P
Monocyte	CD14	0.387	***	0.468	***	-0.032	0.618	0.357	***	0.369	***	0.368	***
	CD86	0.372	***	0.452	***	-0.077	0.226	0.289	***	0.303	***	0.300	***
	CD16(FCGR3A)	0.433	***	0.496	***	0.023	0.720	0.354	***	0.274	***	0.269	***
TAM	CD68	0.302	***	0.392	***	-0.029	0.653	0.329	***	0.123	0.016	0.136	*
	CCL2	0.456	***	0.503	***	0.034	0.590	0.325	***	0.482	***	0.486	***
	CCL5	0.188	***	0.279	***	-0.061	0.337	0.242	***	0.217	***	0.219	***
M1 Macrophage	INOS (NOS2)	0.178	***	0.168	**	0.093	0.145	0.172	*	-0.137	*	-0.123	0.012
	CXCL10	0.111	0.015	0.184	***	-0.235	**	-0.034	0.556	-0.022	0.671	-0.001	0.982
	TNF-α (TNF)	0.048	0.291	0.152	**	-0.015	0.613	0.080	0.167	-0.067	0.194	-0.060	0.222
M2 Macrophage	CD206(MRC1)	0.442	***	0.504	***	0.157	0.013	0.421	***	0.368	***	0.367	***
	CD163	0.471	***	0.534	***	-0.092	0.147	0.398	***	0.367	***	0.366	***
	IL10	0.342	***	0.410	***	0.211	**	0.414	***	0.359	***	0.346	***
Neutrophils	CD66b (CEACAM8)	0.134	*	0.158	**	0.122	0.055	0.074	0.198	-0.028	0.587	-0.019	0.702
	CD11b (ITGAM)	0.436	***	0.502	***	-0.001	0.992	0.341	***	0.416	***	0.410	***
	CCR7	0.343	***	0.429	***	0.058	0.359	0.301	***	0.427	***	0.413	***
	CD15(FUT4)	0.219	***	0.247	***	0.109	0.086	0.197	**	-0.245	***	-0.239	***
Natural killer cell	KIR2DL1	0.092	0.046	0.139	*	0.041	0.519	0.132	0.021	0.087	0.090	0.105	0.032
	KIR2DL3	0.177	**	0.210	***	-0.026	0.687	0.064	0.266	0.025	0.630	0.067	0.171
	KIR2DL4	0.055	0.235	0.114	0.011	-0.236	**	0.007	0.906	-0.157	*	-0.141	*
	KIR3DL1	0.213	***	0.267	***	0.036	0.574	0.180	*	0.064	0.216	0.086	0.082
	KIR3DL2	0.130	*	0.186	***	0.002	0.975	0.141	0.014	0.114	0.027	0.138	*
	KIR3DL3	0.071	0.123	0.095	0.039	0.034	0.593	0.059	0.310	-0.135	*	-0.116	0.018
	KIR2DS4	0.173	**	0.207	***	0.061	0.336	0.149	**	0.003	0.958	0.013	0.799
Dendritic cell	HLA-DPB1	0.399	***	0.476	***	-0.142	0.025	0.169	**	0.247	***	0.249	***
	HLA-DQB1	0.253	***	0.340	***	-0.052	0.413	0.161	**	0.109	0.034	0.120	0.015
	HLA-DRA	0.365	***	0.442	***	-0.166	*	0.104	0.071	0.127	0.013	0.134	*
	HLA-DPA1	0.407	***	0.479	***	-0.148	0.019	0.136	0.018	0.174	**	0.181	**
	BDCA-1(CD1C)	0.263	***	0.372	***	0.014	0.820	0.245	***	0.528	***	0.502	***
	BDCA-4(NRP1)	0.350	***	0.427	***	0.164	*	0.412	***	0.551	***	0.551	***
	CD11c (ITGAX)	0.399	***	0.479	***	-0.003	0.956	0.306	***	0.324	***	0.335	***
	NKp46(NCR1)	0.211	***	0.263	***	-0.003	0.962	0.166	**	0.171	**	0.188	**

LUSC, lung squamous cell carcinoma; OV, ovarian serous cystadenocarcinoma; STAD, stomach adenocarcinoma; TAM, tumor-associated macrophage; Cor, R value of Spearman's correlation; None, correlation without adjustment. Purity, correlation adjusted by purity. *P < 0.01; **P < 0.001; ***P < 0.0001.

Supplementary Table 6. Correlation analysis between PTGIS and relate genes and markers of adaptive immunity cells in TIMER.

Description	Gene markers	LUSC				OV				STAD			
		Purity		None		Purity		None		Purity		None	
		Cor	P	Cor	P	Cor	P	Cor	P	Cor	P	Cor	P
CD8+ T cell	CD8A	0.275	***	0.346	***	0.007	0.918	0.284	***	0.280	***	0.286	***
	CD8B	0.297	***	0.335	***	0.002	0.970	0.222	**	0.220	***	0.215	***
T cell (general)	CD3D	0.239	***	0.339	***	-0.031	0.631	0.278	***	0.188	**	0.189	**
	CD3E	0.318	***	0.409	***	0.000	0.999	0.309	***	0.242	***	0.227	***
	CD2	0.307	***	0.359	***	-0.014	0.831	0.293	***	0.254	***	0.247	***
B cell	CD19	0.344	***	0.438	***	-0.025	0.699	-0.033	0.573	0.365	***	0.348	***
	CD20(MS4A1)	0.334	***	0.428	***	0.164	*	0.326	***	0.408	***	0.401	***
	CD138(SDC1)	-0.171	**	-0.152	**	0.191	*	0.320	***	-0.290	***	-0.297	***
	CD23(FCER2)	0.343	***	0.429	***	0.213	**	0.313	***	0.405	***	0.392	***
Th1	T-bet (TBX21)	0.276	***	0.361	***	-0.046	0.467	0.269	***	0.255	***	0.252	***
	STAT4	0.311	***	0.396	***	0.048	0.446	0.289	***	0.328	***	0.319	***
	STAT1	0.046	0.318	0.119	*	-0.230	**	-0.118	0.041	-0.070	0.172	-0.064	0.196
	IFN-γ (IFNG)	0.076	0.098	0.134	*	-0.125	0.049	0.125	0.029	-0.092	0.074	-0.093	0.057
	TNF-α (TNF)	0.048	0.291	0.152	**	-0.015	0.613	0.080	0.167	-0.067	0.194	-0.060	0.222
Th2	GATA3	0.215	***	0.288	***	0.004	0.946	0.253	***	0.384	***	0.375	***
	STAT6	-0.063	0.170	-0.033	0.462	-0.100	0.115	-0.110	0.055	0.122	0.018	0.129	*
	STAT5A	0.334	***	0.414	***	0.027	0.677	0.136	0.018	0.360	***	0.350	***
	IL13	0.177	***	0.223	***	0.053	0.401	0.072	0.211	0.131	0.010	0.130	*
Tfh	BCL6	0.019	0.685	0.000	0.998	0.000	0.997	-0.027	0.642	0.530	***	0.517	***
	IL21	0.156	**	0.213	***	-0.114	0.073	-0.082	0.154	0.052	0.312	0.049	0.318
	CD278(ICOS)	0.280	***	0.374	***	-0.033	0.606	0.235	***	0.130	0.012	0.132	*
	CXCL13	0.197	***	0.293	***	-0.026	0.680	0.199	**	0.243	***	0.236	***
Th17	STAT3	0.184	***	0.232	***	0.038	0.549	0.222	**	0.363	***	0.365	***
	IL17A	0.038	0.405	0.074	0.097	-0.105	0.097	0.042	0.470	-0.261	***	-0.272	***
Treg	FOXP3	0.350	***	0.429	***	-0.024	0.711	0.240	***	0.241	***	0.244	***
	CCR8	0.381	***	0.453	***	-0.033	0.604	0.130	0.024	0.344	***	0.345	***
	STAT5B	0.262	***	0.264	***	0.269	***	0.275	***	0.603	***	0.608	***
	TGFβ (TGFB1)	0.084	0.067	0.181	***	0.169	*	0.472	***	0.527	***	0.528	***
	CD25(IL2RA)	0.346	***	0.429	***	0.200	*	0.450	***	0.187	**	0.197	***
T cell exhaustion	PD-1 (PDCD1)	0.271	***	0.356	***	-0.106	0.096	0.200	**	0.147	*	0.158	*
	CTLA4	0.253	***	0.349	***	-0.044	0.490	0.240	***	0.088	0.087	0.092	0.062
	LAG3	0.128	*	0.206	***	-0.169	*	0.051	0.373	0.075	0.145	0.080	0.103
	TIM-3 (HAVCR2)	0.390	***	0.464	***	-0.036	0.572	0.336	***	0.291	***	0.294	***
	GZMB	0.144	*	0.236	***	-0.068	0.282	0.203	**	-0.089	0.085	-0.064	0.194

LUSC, lung squamous cell carcinoma; OV, ovarian serous cystadenocarcinoma; STAD, stomach adenocarcinoma; Th, T helper cell; Tfh, Follicular helper T cell; Treg, regulatory T cell; Cor, R value of Spearman's correlation; None, correlation without adjustment. Purity, correlation adjusted by purity. *P < 0.01; **P < 0.001; ***P < 0.0001.

Supplementary Table 7. Correlation analysis between PTGIS and immune relate genes of monocyte and macrophages in GEPIA.

Description	Gene markers	LUSC				OV				STAD			
		Normal		Tumor		Normal		Tumor		Normal		Tumor	
		R	P	R	P	R	P	R	P	R	P	R	P
Monocyte	CD14	0.011	0.86	0.49	***	0.46	***	0.41	***	0.67	***	0.40	***
	CD86	-0.011	0.86	0.46	***	0.41	***	0.36	***	0.49	***	0.33	***
	CD16(FCGR3A)	6E-04	0.99	0.52	***	0.42	***	0.43	***	0.51	***	0.30	***
TAM	CD68	-0.11	0.052	0.42	***	0.39	**	0.4	***	0.44	***	0.19	***
	CCL2	0.085	0.150	0.51	***	0.43	***	0.31	***	0.66	***	0.51	***
	CCL5	0.22	**	0.27	***	0.21	0.044	0.2	***	-0.27	**	0.23	***
M1 Macrophage	INOS (NOS2)	0.19	*	0.18	***	-0.084	0.440	0.36	***	0.63	***	-0.086	0.081
	CXCL10	0.22	**	0.17	**	-0.18	0.095	0.018	0.710	0.03	0.690	0.023	0.640
	TNF-α (TNF)	0.039	0.51	0.15	**	0.13	0.240	0.16	0.001	0.27	**	-0.007	0.890
M2 Macrophage	CD206(MRC1)	-0.06	0.33	0.53	***	0.37	**	0.51	***	0.67	***	0.40	***
	CD163	-0.13	0.033	0.53	***	0.32	*	0.36	***	0.60	***	0.37	***
	IL10	0.029	0.620	0.42	***	0.44	***	0.49	***	0.62	***	0.38	***

LUSC, lung squamous cell carcinoma; OV, ovarian serous cystadenocarcinoma; STAD, stomach adenocarcinoma. TAM, Tumor-associated macrophages. Tumor, correlation analysis in tumor tissue of TCGA. Normal, correlation analysis in normal tissue of GTEx. *P < 0.01; **P < 0.001; ***P < 0.0001.